Title
Modeling And Control Of Articulated Vehicles

Permalink
https://escholarship.org/uc/item/2k64h8k3

Authors
Chen, Chieh
Tomizuka, Masayoshi

Publication Date
1997

This paper has been mechanically scanned. Some errors may have been inadvertently introduced.

Modeling and Control of Articulated Vehicles

Chieh Chen
Masayoshi Tomizuka
University of California, Berkeley

Dynamic Modeling and Lateral Control of Articulated Vehicles

Chieh Chen and Masayoshi Tomizuka

Department of Mechanical Engineering
University of California at Berkeley

Abstract

A control oriented dynamic modeling approach for articulated vehicles is proposed. A generalized coordinate system is introduced to describe the kinematics of the vehicle. Equations of motion of a tractor-semitrailer vehicle are derived based on the Lagrange mechanics. Experimental studies are conducted to validate the effectiveness of this modeling approach. Two nonlinear lateral control algorithms are designed for a tractor-semitrailer vehicle. The baseline steering control algorithm is designed utilizing input-output linearization. To prevent jackknifing and furthermore reduce tracking errors of the trailer, braking forces are independently controlled on the inner and outer wheels of the trailer. The coordinated steering and braking control algorithm is designed based on the multivariable backstepping technique. Simulations show that the trailer yaw errors under coordinated steering and independent braking force control are smaller than those without independent braking force control.

Keywords

Dynamic Modeling, Advanced Vehicle Control Systems, Lateral control, Steering Control, Braking Control

Executive Summary

This report summarizes and concludes the research results on lateral control of Commercial Heavy Vehicles in Automated Highway Systems (AHS) conducted in the multi-year PATH project MOU129-242: Steering and Braking Control of Heavy Duty Vehicles. Under this project, dynamic modeling of single unit as well as articulated heavy vehicles was done. Several linear and nonlinear control techniques were designed for the lateral guidance. Extensive simulation studies were conducted to verify the effectiveness of the control strategies. The next stage of this research, the experimental validation, will be continued under the path project MOU 313: Lateral Control of Commercial Heavy Vehicles.

The work done under MOU 242 is reported in two parts. Part I of the report "Modeling and Control of Articulated Vehicles" is presented here. The second part "Lateral Control of Single Unit Heavy Vehicles", which is concerned with the robustness and performance specification and the design of lateral controllers for Single-Unit heavy vehicles, is presented in another separate report.

In this report, two types of dynamic models of tractor-semitrailer vehicles are utilized for the analysis and design of lateral controllers. The first type of dynamic model is a complex simulation model. The second type of dynamic models are two simplified control models, which are derived from the complex nonlinear model. This modeling approach utilizes Lagrangian mechanics and has an advantage over the Newtonian mechanics formulation in that this complex model eliminates the holonomic constraint at the fifth wheel (linking joint) by choosing the generalized coordinates. Since there is no constraint involved in the equations of motion, it is easier to design control algorithms and solve the differential equations numerically. The effectiveness of this modeling approach is shown by comparing the experimental results of a tractor-semitrailer vehicle with the simulation results of the complex tractor-semitrailer vehicle model.

Two control algorithms for lateral guidance of tractor-semitrailer vehicles are designed. The first is a baseline steering control algorithm and the second is a coordinated steering and independent braking control algorithm. In the design of the second control algorithm, we utilize tractor front wheel steering angles and trailer independent braking forces to control the tractor and the trailer motion. The multivariable backstepping design methodology is utilized to determine the coordinated steering angle and braking torques on the trailer wheels. Simulations show that both the tractor and the trailer yaw errors under coordinated steering and independent braking force control are smaller than those without independent braking force control.

1   Introduction

This report is concerned with dynamic modeling and lateral control of commercial heavy-duty vehicles for highway automation.

In the past, automatic vehicle control research work for Automated Highway Systems (AHS) have been emphasized on passenger vehicles (Fenton 1991, Shladover et. al. 1991, Peng and Tomizuka 1993). Less attention, however, has been paid to control issues of commercial heavy vehicles for AHS. The study of heavy vehicles for AHS applications has gained interest only recently (Bishel 1993, Chen and Tomizuka 1995, Favre 1995, Kanellakopoulos and Tomizuka 1996, Yanakiev and Kanellakopoulos 1995, Zimmermann 1994). On the other hand, the study of lateral guidance of heavy-duty vehicles is important for several reasons. In 1993, the share of the highway miles accounted for by truck traffic was around 28% (Federal Highway Administration 1994). This is a significant percentage of the total highway miles traveled by all the vehicles in US. According to Motor Vehicles Facts and Figures (American Automobile Manufactures' Association 1993), the total number of registered trucks (light, commercial and truck-trailer combinations) formed approximately 10% of the national figures in 1991 and **30.9%** of the highway taxes came from heavy vehicles. Also, due to several economic and policy issues, heavy vehicles have the potential of becoming the main beneficiaries of automated guidance (Kanellakopoulos and Tomizuka 1996). The main reasons are:

- *o* On average, a truck travels six times the miles **as** compared to a passenger vehicle. Possible reduction in the number of drivers will reduce the operating cost substantially.

- *o* Relative equipment cost for automating heavy vehicles is far less than for passenger vehicles.

- *o* Automation of heavy vehicles will have a significant impact on the overall safety of the automated guidance system. Trucking is a tedious job and automation will contribute positively to reducing driving stress and thereby increase safety.

Thus commercial heavy vehicles will gain significant benefit from Advanced Vehicle Control Systems (AVCS), and may actually become automated earlier than passenger vehicles due to economical considerations.

Due to the popularity of the tractor-semitrailer type commercial heavy-duty vehicle, we will use it **as** the benchmark vehicle in our study. Two types of dynamic models are developed in the study of lateral control of tractor-semitrailer vehicles in AHS: a complex simulation model and two simplified control models. In this report, a nonlinear complex model is developed to simulate the dynamic responses of tractor-semitrailer

1

vehicles and will be exploited to evaluate the effectiveness of lateral control algorithms. This simulation model consists of three main components: the vehicle sprung mass (body) dynamics, a tire model and a suspension model. The main distinction between this complex model and those in the literatures is that the vehicle sprung mass dynamics is derived by applying Lagrangian mechanics. This approach has an advantage over a Newtonian mechanics formulation in that this modeling approach eliminates the holonomic constraint at the fifth wheel of the tractor-semitrailer vehicle by choosing the articulation angle as the generalized coordinate. Since there is no constraint involved in the model, it is easier for both designing control algorithms and solving the differential equations numerically. Other configurations of articulated vehicles, for example the tractor/three trailer combination, can also be modeled with the same approach.

The second type of dynamic models are represented by two simplified lateral control models: one for steering control and the other for coordinated steering and differential braking control. These lateral control models, which are simplified from the complex model, will be developed.

A steering control algorithm using input/output linearization is designed as a baseline controller to achieve the lane following maneuver in AHS. As safety is always of primary concern in AHS, a coordinated steering-independent braking control algorithm is considered to enhance driving safety and avoid unstable trailer yaw motion. This coordinated steering and braking control algorithm utilizes the tractor front wheel steering and the braking force at each of the rear trailer wheels as control inputs. Simulation studies using the complex vehicle model will be conducted to show the performance of the coordinated steering and independent braking control strategy.

The organization of this report is as follows. In section 2, a coordinate system is introduced to describe the motion of the tractor-semitrailer type commercial heavy-duty vehicles. Based on the coordinate system in section 2, the kinetic energy and the potential energy are calculated in section **3.** In section **4,** a set of equations describing the sprung mass dynamics are derived by using Lagrange's mechanics. In conjunction with the equations of the unsprung mass dynamics, the expression of the generalized force corresponding to each coordinate is obtained in section 5. To complete the development of the complex model, we present the tire model by (Baraket and Fancher 1989) and a simplified suspension model in section 6. Effectiveness of this modeling approach is shown in section **7** by comparing the open loop experimental results of a tractor-semitrailer vehicle and the simulation results from the complex model. In section 8, the transformation relationships between the road reference coordinate and the vehicle unsprung mass reference coordinate are explored and will be used to obtain control models. In section 9, a steering control model is formulated. Based on this model, a baseline steering Controller is designed in section 10. **A** steering and braking control model is formulated in section **11** and the coordinated steering and braking control algorithm is designed in section 12. Conclusions of this report are given in the last section.

2 Definition of Coordinate System
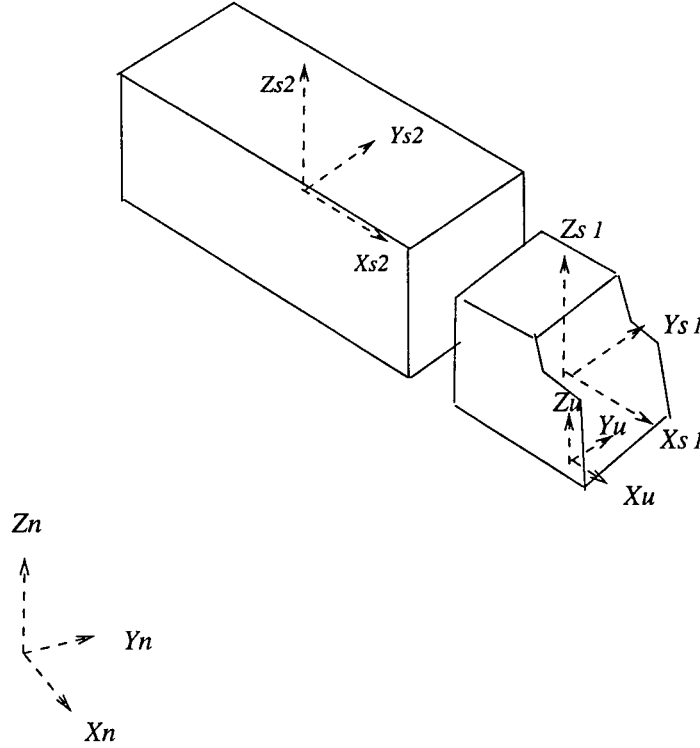
2.1 Coordinate System

Figure 1: Coordinate System to Describe the Vehicle Motion

A coordinate system is defined to characterize the motion of a tractor-semitrailer type of articulated vehicle. As shown in Fig. 1, $X_n Y_n Z_n$ is the globally fixed inertial reference coordinate. We will obtain the expressions of vehicle kinetic and potential energies with respect to this reference coordinate. $X_u Y_u Z_u$ is the tractor's unsprung mass coordinate, which has the same orientation as the tractor. The Z_u axis passes through the tractor's C.G. The translational motion of the tractor in the X, $-Y_n$ plane and the yaw motion of the tractor along the Z_n axis can be described by the relative motion of the $X_u Y_u Z_u$ coordinate with respect to $X_n Y_n Z_n$. $X_{s1} Y_{s1} Z_{s1}$ is the tractor's sprung mass coordinate, which is body-fixed at the tractor's center of gravity. Coordinate $X_{s1} Y_{s1} Z_{s1}$ has roll motion relative to coordinate $X_u Y_u Z_u$. The trailer's motion can be characterized by describing the articulation angle between the tractor and the trailer, or the relative motion of the trailer's unsprung mass coordinate $X_{s2} Y_{s2} Z_{s2}$ with respect to the tractor's unsprung mass coordinate $X_{s1} Y_{s1} Z_{s1}$. Having defined the coordinate systems, a set of state variables for the tractor-semitrailer vehicle can be introduced as

- $x_{,,}$: *position of the tractor* C.G. *in X*, *direction of the inertial coordinate* $X_n Y_n Z_n$
- $\dot{x}_n$: *velocity of the tractor* C.G. *in X*, *direction of the inertial coordinate* $X_n Y_n Z_n$

3

- y_n : *position of the tmctor C.G. in Y_n direction of the inertial coordinate $X_n Y_n Z_n$*

- $\dot{y}_n$: *velocity of the tmctor C.G. in Y_n direction of the inertial coordinate $X_n Y_n Z_n$*

- ϵ_1 : *tractor yaw angle with respect to inertial coordinate $X_n Y_n Z_n$*

- $\dot{\epsilon}_1$: *tractor yaw rate with respect to inertial coordinate $X_n Y_n Z_n$*

- ϕ : *tractor roll angle*

- $\dot{\phi}$: *mte of change of tmctor roll angle*

- ϵ_f : *articulation angle between the tractor and the tmiler*

- $\dot{\epsilon}_f$: *rate of change of the articulation angle between the tractor and the trailer*

With the definition of the state variables, we can calculate the transformation matrices between those coordinates. The transformation matrices will be used to obtain the kinematics of the vehicle. The transformation matrices between the inertial reference frame and the unsprung mass coordinate are

$$
\begin{pmatrix} i_n \\ j_n \\ k_n \end{pmatrix} = \begin{pmatrix} cos\epsilon_1 & -sin\epsilon_1 & 0 \\ sin\epsilon_1 & cos\epsilon_1 & 0 \\ 0 & 0 & 1 \end{pmatrix} \begin{pmatrix} i_u \\ j_u \\ k_u \end{pmatrix} \tag{1}
$$

and

$$
\begin{pmatrix} i_u \\ j_u \\ k_u \end{pmatrix} = \begin{pmatrix} cos\epsilon_1 & sin\epsilon_1 & 0 \\ -sin\epsilon_1 & cos\epsilon_1 & 0 \\ 0 & 0 & 1 \end{pmatrix} \begin{pmatrix} i_n \\ j_n \\ k_n \end{pmatrix} \tag{2}
$$

The transformation matrices between the unsprung mass coordinate and the tractor's sprung mass coordinate are

$$
\begin{pmatrix} i_u \\ j_u \\ k_u \end{pmatrix} = \begin{pmatrix} 1 & & 0 \\ 0 & \phi & -\phi \\ 0 & & 1 \end{pmatrix} \begin{pmatrix} i_{s1} \\ j_{s1} \\ k_{s1} \end{pmatrix} \tag{3}
$$

and

$$
\begin{pmatrix} i_{s1} \\ j_{s1} \\ k_{s1} \end{pmatrix} = \begin{pmatrix} 1 & 0 & 0 \\ 0 & -1\phi & \phi \\ 0 & & 1 \end{pmatrix} \begin{pmatrix} i_u \\ j_u \\ k_u \end{pmatrix} \tag{4}
$$

The transformation matrices between the tractor's sprung mass coordinate and the trailer's sprung mass coordinate are

$$
\begin{pmatrix} i_{s1} \\ j_{s1} \\ k_{s1} \end{pmatrix} = \begin{pmatrix} cos\epsilon_f & -sin\epsilon_f & 0 \\ sin\epsilon_f & cos\epsilon_f & 0 \\ 0 & 0 & 1 \end{pmatrix} \begin{pmatrix} i_{s2} \\ j_{s2} \\ k_{s2} \end{pmatrix} \tag{5}
$$

4

and

$$\begin{pmatrix} \mathbf{i_{s2}} \\ \mathbf{j_{s2}} \\ \mathbf{k_{s2}} \end{pmatrix} = \begin{pmatrix} cos\epsilon_f & sin\epsilon_f & 0 \\ -sin\epsilon_f & cos\epsilon_f & 0 \\ 0 & 0 & 1 \end{pmatrix} \begin{pmatrix} \mathbf{i_{s1}} \\ \mathbf{j_{s1}} \\ \mathbf{k_{s1}} \end{pmatrix}. \tag{6}$$
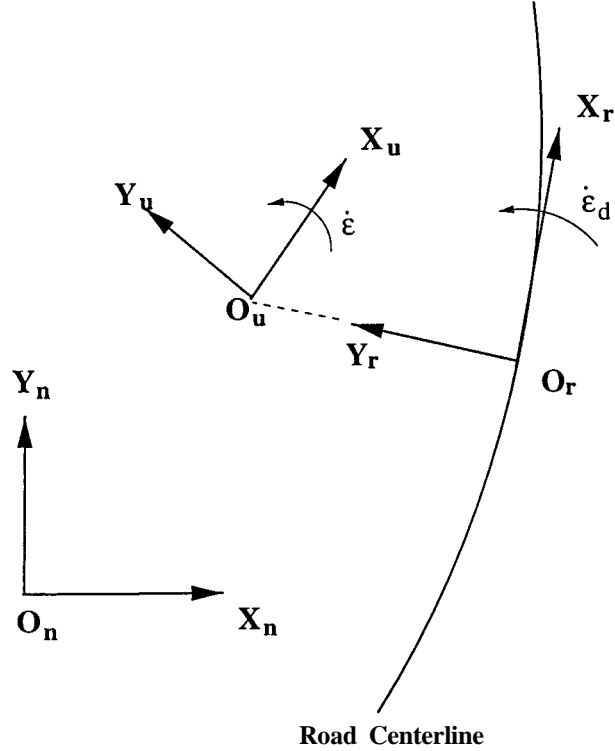
2.2 Reference Frame

Figure 2: Three Reference Coordinates

As shown in Fig.2, three types of reference frames are used to describe the translational and rotational motion of vehicles. They are inertial reference frame $X_n Y_n Z_n$, vehicle unsprung mass reference frame $X_u Y_u Z_u$ and road reference frame $X_r Y_r Z_r$. In this report the complex vehicle model is first derived with respect to the inertial reference frame. However, state variables, such as the position and the orientation, of a vehicle with respect to the inertial reference frame are not what we are concerned with. The complex model is transformed so that it depends only on state variables with respect to the unsprung mass reference frame. The vehicle model relative to the unsprung mass reference frame does not depend explicitly on the position and the orientation of the vehicle. This is widely used in vehicle dynamics to predict and analyze vehicle handling response, since the side slip angle, yaw rate and lateral acceleration of the vehicle are naturally defined in this reference frame. Further, for the lane following manever in automated highway

5

systems, the road reference coordinate $OrXrYr$ in Fig.:! is naturally introduced to describe tracking errors of the vehicle with respect to the road centerline. The road reference coordinate $OrXrYr$ is such defined that the X,. axis is tangent to the road centerline and the Y_r axis passes through the center of gravity of the vehicle. By studing the kinematics with respect to different reference frames, transformations from the inertial reference frame to the unsprung mass reference frame and from the unsprung mass reference frame to the road reference frame will be obtained. In the following section, the transformation between the inertial reference frame and the unsprung mass reference frame will be studied. It will be used in section 4 to obtain the complex vehicle model. The transformation between the unsprung mass reference frame and the road reference frame will be studied to obtain control models.

2.3 Transformation between the inertial reference frame and the unsprung mass reference frame
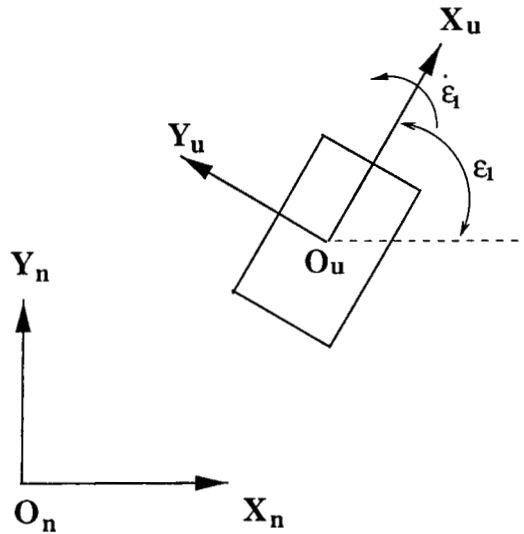

Figure 3: Inertial and Unsprung Mass Reference Frames

From Fig. 3, the vehicle velocity at C.G. with respect to the inertial reference frame is

$$\mathbf{V_{CG}} = \dot{x}_n \mathbf{i_n} + \dot{y}_n \mathbf{j_n} \tag{7}$$

where $\dot{x}_n$ is the component of the vehicle velocity along the X, axis and $\mathbf{y}$ is the component of the vehicle velocity along the Y_n axis. The vehicle acceleration at C.G. can be obtained by differentiating Eq. (7),

$$\mathbf{a_{CG}} = \ddot{x}_n \mathbf{i_n} + \ddot{y}_n \mathbf{j_n}. \tag{8}$$

On the other hand, the vehicle velocity at C.G. can also be denoted as

$$\mathbf{V_{CG}} = \dot{x}_u \mathbf{i_u} + \dot{y}_u \mathbf{j_u}, \tag{9}$$

6

where $\dot{x}_u$ is the velocity component along the X_u axis of the unsprung mass coordinate and $\dot{y}_u$ is the velocity component along the Y_u axis of the unsprung mass coordinate. Then the vehicle acceleration at C.G. can be obtained by differentiating Eq. (9),

$$\begin{aligned}
\mathbf{a_{CG}} &= \ddot{x}_u \mathbf{i_u} + \dot{x}_u \tfrac{d}{dt}\mathbf{i_u} + \ddot{y}_u \mathbf{j_u} + \dot{y}_u \tfrac{d}{dt}\mathbf{j_u} \\
&= (\ddot{x}_u - \dot{y}_u \dot{\epsilon}_1)\mathbf{i_u} + (\ddot{y}_u + \dot{x}_u \dot{\epsilon}_1)\mathbf{j_u},
\end{aligned} \tag{10}$$

where

$$\frac{d}{dt}\mathbf{i_u} = \dot{\epsilon}_1 \mathbf{j_u}$$

and

$$\frac{d}{dt}\mathbf{j_u} = -\dot{\epsilon}_1 \mathbf{i_u}$$

are used in Eq. (10). By equating Eqs. (7) and (9) and noting the transformation matrix

$$\begin{pmatrix} \mathbf{i_n} \\ \mathbf{j_n} \end{pmatrix} = \begin{pmatrix} cos\ \epsilon_1 & -sin\ \epsilon_1 \\ sin\ \epsilon_1 & cos\ \epsilon_1 \end{pmatrix} \begin{pmatrix} \mathbf{i_u} \\ \mathbf{j_u} \end{pmatrix}, \tag{11}$$

we have

$$\begin{aligned}
(\dot{x}_u\ \ \dot{y}_u) \begin{pmatrix} \mathbf{i_u} \\ \mathbf{j_u} \end{pmatrix} &= (\dot{x}_n\ \ \dot{y}_n) \begin{pmatrix} \mathbf{i_n} \\ \mathbf{j_n} \end{pmatrix} \\
&= (\dot{x}_n\ \ \dot{y}_n) \begin{pmatrix} cos\ \epsilon_1 & -sin\ \epsilon_1 \\ sin\ \epsilon_1 & cos\ \epsilon_1 \end{pmatrix} \begin{pmatrix} \mathbf{i_u} \\ \mathbf{j_u} \end{pmatrix}
\end{aligned} \tag{12}$$

or

$$\dot{x}_n\ cos\ \epsilon_1 + \dot{y}\ sin\ \epsilon_1 = \dot{x}_u \tag{13}$$

$$-\dot{x}_n\ sin\ \epsilon_1 + \dot{y}_n\ cos\ \epsilon_1 = \dot{y}_u. \tag{14}$$

Similarly, by equating Eqs. (8) and (10) and using the transformation matrix (11), we obtain

$$\begin{aligned}
(\ddot{x}_u - \dot{y}_u \dot{\epsilon}_1\ \ \ddot{y}_u + \dot{x}_u \dot{\epsilon}_1) \begin{pmatrix} \mathbf{i_u} \\ \mathbf{j_u} \end{pmatrix} &= (\ddot{x}_n\ \ \ddot{y}_n) \begin{pmatrix} \mathbf{i_n} \\ \mathbf{j_n} \end{pmatrix} \\
&= (\ddot{x}_n\ \ \ddot{y}_n) \begin{pmatrix} cos\ \epsilon_1 & -sin\ \epsilon_1 \\ sin\ \epsilon_1 & cos\ \epsilon_1 \end{pmatrix} \begin{pmatrix} \mathbf{i_u} \\ \mathbf{j_u} \end{pmatrix},
\end{aligned} \tag{15}$$

or

$$\ddot{x}_n cos\ \epsilon_1 + \ddot{y}_n sin\ \epsilon_1 = \ddot{x}_u - \dot{y}_u \dot{\epsilon}_1 \tag{16}$$

$$-\ddot{x}_n sin\ \epsilon_1 + \ddot{y}_n cos\ \epsilon_1 = \ddot{y}_u + \dot{x}_u \dot{\epsilon}_1. \tag{17}$$

Eqs. (13), (14), (16) and (17) will be used to transform equations of motion from the inertial reference frame to the unsprung mass reference frame.

3 Vehicle Kinematics

In this section, translational and rotational velocities will be calculated for both the tractor and the trailer. Then the expressions of kinetic energy and potential energy that will be used to derive the vehicle model by applying Lagrange's equations in section **4,** are given. Vehicle parameters are depicted in Fig. 4 and listed in Table 1.
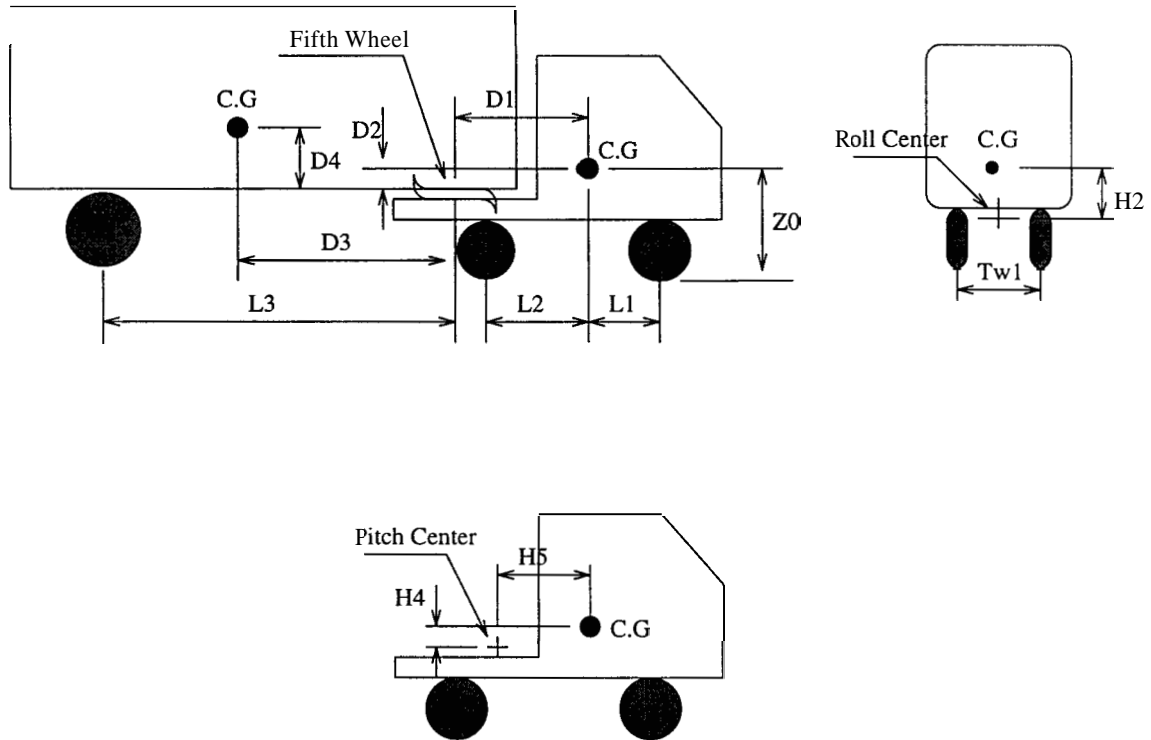
Figure **4:** Schematic Diagram of Complex Vehicle Model

3.1 Tractor Kinematics

To facilitate the calculation of the tractor translational velocity, several identities of time derivatives of unit vectors in each coordinate frame will be established in this section. These identities include the time derivatives of the unit vectors along the X, Y, and Z axis of the unsprung mass coordinate and the sprung mass coordinate. Recall that the angular velocity of the tractor's unsprung mass coordinate is

$$\omega_{\mathbf{u/n}} = \dot{\epsilon}_1 \mathbf{k_u}. \tag{18}$$

parameter	description
m_1	tractor's mass
I_{x1}, I_{y1}, I_{z1}	tractor's moment of inertia
m_2	semitrailer's mass
I_{x2}, I_{y2}, I_{z2}	semitrailer's moment of inertia
l_1	distance between tractor C.G. and front wheel axle
l_2	distance between tractor C.G. and real wheel axle
l_3	distance between joint (fifth wheel) and trailer real wheel axle
d_1, d_2	relative position between tractor's C.G. to fifth wheel
d_3, d_4	relative position between semitrailer's C.G. to fifth wheel
T_{w1}	tractor front axle track width
T_{w2}	tractor rear axle track width
T_{w3}	semitrailer rear axle track width
h_2	distance from tractor roll center to C.G.
$C_{\alpha f}$	cornering stiffness of tractor front wheel
$C_{\alpha r}$	cornering stiffness of tractor rear wheel
$C_{\alpha t}$	cornering stiffness of semitrailer rear wheel
Sx_f	longitudinal stiffness of tractor front wheel
Sx_r	longitudinal stiffness of tractor rear wheel
Sx_t	longitudinal stiffness of semitrailer rear wheel

Table 1: Parameters of Complex Vehicle Model

Thus the derivatives of the unit vectors in the unsprung mass coordinate are

$$\frac{d}{dt}\mathbf{i_u} = \omega_{u/n} \times \mathbf{i_u} = \dot{\epsilon}_1 \mathbf{j_u} \tag{19}$$

$$\frac{d}{dt}\mathbf{j_u} = \omega_{u/n} \times \mathbf{j_u} = -\dot{\epsilon}_1 \mathbf{i_u} \tag{20}$$

and

$$\frac{d}{dt}\mathbf{k_u} = \omega_{u/n} \times \mathbf{k_u} = 0, \tag{21}$$

respectively. Since the sprung mass coordinate has relative roll motion with respect to the unsprung mass coordinate, the angular velocity of the sprung mass coordinate $X_{s1}Y_{s1}Z_{s1}$ is

$$\begin{aligned}
\omega_{s1/n} &= \omega_{s1/u} + \omega_{u/n} \\
&= \dot{\phi}\mathbf{i_{s1}} + \dot{\epsilon}_1 \mathbf{k_u} \\
&= \dot{\phi}\mathbf{i_{s1}} + \dot{\phi}\epsilon_1 \mathbf{j_{s1}} + \dot{\epsilon}_1 \mathbf{k_{s1}},
\end{aligned} \tag{22}$$

9

where

$$k_u = \phi \dot{j}_{s1} + k_{s1} \tag{23}$$

is used in (22). Then the derivatives of the unit vectors in the sprung mass coordinate are

$$\frac{d}{dt} i_{s1} = \omega_{s1/n} \times i_{s1} = \dot{\epsilon}_1 j_{s1} - \phi \dot{\epsilon}_1 k_{s1} \tag{24}$$

$$\frac{d}{dt} j_{s1} = \omega_{s1/n} \times j_{s1} = -\dot{\epsilon}_1 i_{s1} + \dot{\phi} k_{s1} \tag{25}$$

and

$$\frac{d}{dt} k_{s1} = \omega_{s1/n} \times k_{s1} = \phi \dot{\epsilon}_1 i_{s1} - \dot{\phi} j_{s1}, \tag{26}$$

respectively. Eqs. (19), (20), (21), (24), (25) and (26) will be used in the following to calculate translational velocity of the tractor.

Translational Velocity at Tractor *C.G.*

Fron Fig. 4 the position of the tractor *C.G* can be expressed as

$$
\begin{aligned}
r_{CG1/n} &= r_{CG1/u} + r_{u/n} \\
&= z_0 k_u + h_2 k_{s1} + x_n i_n + y_n j_n.
\end{aligned} \tag{27}
$$

By differentiating (27), the velocity of the tractor C.G. is obtained as

$$
\begin{aligned}
v_{CG1/n} &= \dot{x}_n i_n + \dot{y}_n j_n + h_2 \frac{d}{dt} k_{s1} \\
&= \dot{x}_n i_n + \dot{y}_n j_n + h_2 \phi \dot{\epsilon}_1 i_{s1} - h_2 \dot{\phi} j_{s1} \\
&= (\dot{x}_n cos\epsilon_1 + \dot{y}_n sin\epsilon_1) i_u + (-\dot{x}_n sin\epsilon_1 + \dot{y}_n cos\epsilon_1) j_u + h_2 \phi \dot{\epsilon}_1 i_{s1} - h_2 \dot{\phi} j_{s1} \\
&= (\dot{x}_n cos\epsilon_1 + \dot{y}_n sin\epsilon_1 + h_2 \phi \dot{\epsilon}_1) i_{s1} \\
&\quad + (-\dot{x}_n sin\epsilon_1 + \dot{y}_n cos\epsilon_1 - h_2 \dot{\phi}) j_{s1} \\
&\quad + (\dot{x}_n sin\epsilon_1 - \dot{y}_n cos\epsilon_1) \phi k_{s1},
\end{aligned} \tag{28}
$$

where coordinate transformations are used in (28).

3.2 Trailer Kinematics

The angular velocity of trailer unsprung mass coordinate $X_{s2} Y_{s2} Z_{s2}$ is

$$
\begin{aligned}
\omega_{s2/n} &= \omega_{s1} + \dot{\epsilon}_f k_{s2} \\
&= \dot{\phi} i_{s1} + \phi \dot{\epsilon}_1 j_{s1} + \dot{\epsilon}_1 k_{s1} + \dot{\epsilon}_f k_{s2} \\
&= (\dot{\phi} cos\epsilon_f + \phi \dot{\epsilon}_1 sin\epsilon_f) i_{s2} \\
&\quad + (-\dot{\phi} sin\epsilon_f + \phi \dot{\epsilon}_1 cos\epsilon_f) j_{s2} \\
&\quad + (\dot{\epsilon}_1 + \dot{\epsilon}_f) k_{s2}
\end{aligned} \tag{29}
$$

10

Thus the time derivatives of the unit vectors along the X, Y, and Z axis are

$$\frac{d}{dt}\mathbf{i_{s2}} = \omega_{s2/n} \times \mathbf{i_{s2}} = (\dot{\epsilon}_1 + \dot{\epsilon}_f)\mathbf{j_{s2}} + (\dot{\phi}sin\epsilon_f - \phi\dot{\epsilon}_1 cos\epsilon_f)\mathbf{k_{s2}} \tag{30}$$

$$\frac{d}{dt}\mathbf{j_{s2}} = \omega_{s2/n} \times \mathbf{j_{s2}} = -(\dot{\epsilon}_1 + \dot{\epsilon}_f)\mathbf{i_{s2}} + (\dot{\phi}cos\epsilon_f + \phi\dot{\epsilon}_1 sin\epsilon_f)\mathbf{k_{s2}} \tag{31}$$

and

$$\frac{d}{dt}\mathbf{k_{s2}} = \omega_{s2/n} \times \mathbf{k_{s2}} = (-\dot{\phi}sin\epsilon_f + \phi\dot{\epsilon}_1 cos\epsilon_f)\mathbf{i_{s2}} - (\dot{\phi}cos\epsilon_f + \phi\dot{\epsilon}_1 sin\epsilon_f)\mathbf{j_{s2}}, \tag{32}$$

respectively. Eqs. (30), (31) and (32) will be used in the following to calculate the translational velocity at the trailer C.G.

Translational Velocity at the Trailer C.G.

From Fig. **4,** it is easy to see that the position vector of the trailer C.G. can be decomposed into three components as

$$\mathbf{r_{CG2/n}} = \mathbf{r_{CG1/n}} + \mathbf{r_{fw/CG1}} + \mathbf{r_{CG2/fw}} \tag{33}$$

where $\mathbf{r_{CG1/n}}$ is the position vector of the tractor C.G., $\mathbf{r_{fw/CG1}}$ is the position vector from the tractor C.G. to the fifth wheel, and $\mathbf{r_{CG2/fw}}$ is the position vector from the fifth wheel to the trailer C.G. By substituting vehicle geometric parameters into **(33)**, we obtain

$$\mathbf{r_{CG2/n}} = \mathbf{r_{CG1/n}} - d_1\mathbf{i_{s1}} - d_2\mathbf{k_{s1}} - d_3\mathbf{i_{s2}} + d_4\mathbf{k_{s2}}. \tag{34}$$

Consequently, the velocity vector at trailer C.G. can be obtained by differentiating **(34)**,

$$\mathbf{v_{CG2/n}} = \mathbf{v_{CG1/n}} - d_1\frac{d}{dt}\mathbf{i_{s1}} - d_2\frac{d}{dt}\mathbf{k_{s1}} - d_3\frac{d}{dt}\mathbf{i_{s2}} + d_4\frac{d}{dt}\mathbf{k_{s2}} \tag{35}$$

Substituting identities of derivatives of unit vectors (24), (26), (30) and (32) into (35), we obtain

$$
\begin{aligned}
\mathbf{v_{CG2/n}} = & \ (\dot{x}_n cos\epsilon_1 + \dot{y}_n sin\epsilon_1 + h_2\phi\dot{\epsilon}_1)\mathbf{i_{s1}} + (-\dot{x}_n sin\epsilon_1 + \dot{y}_n cos\epsilon_1 - h_2\dot{\phi})\mathbf{j_{s1}} \\
& + (\dot{x}_n sin\epsilon_1 - \dot{y}_n cos\epsilon_1)\phi\mathbf{k_{s1}} - d_1\dot{\epsilon}_1\mathbf{j_{s1}} + d_1\phi\dot{\epsilon}_1\mathbf{k_{s1}} - d_2\phi\dot{\epsilon}_1\mathbf{i_{s1}} + d_2\dot{\phi}\mathbf{j_{s1}} \\
& - d_3(\dot{\epsilon}_1 + \dot{\epsilon}_f)\mathbf{j_{s2}} - d_3(\dot{\phi}sin\epsilon_f - \phi\dot{\epsilon}_1 cos\epsilon_f)\mathbf{k_{s2}} + d_4(-\dot{\phi}sin\epsilon_f + \phi\dot{\epsilon}_1 cos\epsilon_f)\mathbf{i_{s2}} \\
& - d_4(\dot{\phi}cos\epsilon_f + \phi\dot{\epsilon}_1 sin\epsilon_f)\mathbf{j_{s2}} \\
= & \ (\dot{x}_n cos\epsilon_1 + \dot{y}_n sin\epsilon_1 + h_2\phi\dot{\epsilon}_1 - d_2\phi\dot{\epsilon}_1)\mathbf{i_{s1}} \\
& + (-\dot{x}_n sin\epsilon_1 + \dot{y}_n cos\epsilon_1 - h_2\dot{\phi} - d_1\dot{\epsilon}_1 + d_2\dot{\phi})\mathbf{j_{s1}} \\
& + (\dot{x}_n sin\epsilon_1 - \dot{y}_n cos\epsilon_1 + d_1\dot{\epsilon}_1)\phi\mathbf{k_{s1}} \\
& + d_4(-\dot{\phi}sin\epsilon_f + \phi\dot{\epsilon}_1 cos\epsilon_f)\mathbf{i_{s2}} \\
& - (d_3(\dot{\epsilon}_1 + \dot{\epsilon}_f) + d_4(\dot{\phi}cos\epsilon_f + \phi\dot{\epsilon}_1 sin\epsilon_f))\mathbf{j_{s2}} \\
& - d_3(\dot{\phi}sin\epsilon_f - \phi\dot{\epsilon}_1 cos\epsilon_f)\mathbf{k_{s2}}.
\end{aligned} \tag{36}
$$

11

3.3 Kinetic Energy and Potential Energy

Kinetic Energy

The kinetic energy of the tractor-semitrailer vehicle can be obtained by adding the kinetic energy component of the tractor and that of the trailer. The kinetic energy of the tractor, which is denoted as T_1, can be calculated from the translational velocity of the tractor at $\boldsymbol{C.G.}$ and the angular velocity of the tractor's unsprung mass coordinate,

$$T_1 = \frac{1}{2}m_1 \mathbf{v_{CG1}} \cdot \mathbf{v_{CG1}} + \frac{1}{2}\omega_{s1} \cdot I_1 \cdot \omega_{s1} \tag{37}$$

By substituting $\mathbf{v_{CG1}}$ in (28) and ω_{s1} in (22) into (37), we obtain

$$
\begin{aligned}
T_1 = \ & \tfrac{1}{2}m_1(\dot{x}_n cos\epsilon_1 + \dot{y}_n sin\epsilon_1 + h_2\phi\dot{\epsilon}_1)^2 \\
& + \tfrac{1}{2}m_1(-\dot{x}_n sin\epsilon_1 + \dot{y}_n cos\epsilon_1 - h_2\dot{\phi})^2 \\
& + \tfrac{1}{2}m_1((\dot{x}_n sin\epsilon_1 - \dot{y}_n cos\epsilon_1)\phi)^2 \\
& + \tfrac{1}{2}I_{x1}(\dot{\phi})^2 + \tfrac{1}{2}I_{y1}(\phi\dot{\epsilon}_1)^2 + \tfrac{1}{2}I_{z1}(\dot{\epsilon}_1)^2.
\end{aligned}
\tag{38}
$$

Similarly, the kinetic energy of the trailer, denoted as $T2$, can be obtained from the translational velocity at the trailer $\boldsymbol{C.G.}$ and the angular velocity of the trailer's sprung mass coordinate, or

$$T_2 = \frac{1}{2}m_2 \mathbf{v_{CG2}} \cdot \mathbf{v_{CG2}} + \frac{1}{2}\omega_{s2} \cdot I_2 \cdot \omega_{s2} \tag{39}$$

By substituting $\mathbf{v_{CG2}}$ in (36) and ω_{s2} in (29) into (39), we obtain

$$
\begin{aligned}
T_2 = \ & \tfrac{1}{2}m_2(\dot{x}_n cos\epsilon_1 + \dot{y}_n sin\epsilon_1 + h_2\phi\dot{\epsilon}_1 - d_2\phi\dot{\epsilon}_1)^2 \\
& + \tfrac{1}{2}m_2(-\dot{x}_n sin\epsilon_1 + \dot{y}_n cos\epsilon_1 - h_2\dot{\phi} - d_1\dot{\epsilon}_1 + d_2\dot{\phi})^2 \\
& + \tfrac{1}{2}m_2(\dot{x}_n sin\epsilon_1 - \dot{y}_n cos\epsilon_1 + d_1\dot{\epsilon}_1)^2\phi^2 \\
& + \tfrac{1}{2}m_2 d_4^2(-\dot{\phi}sin\epsilon_f + \phi\dot{\epsilon}_1 cos\epsilon_f)^2 \\
& + \tfrac{1}{2}m_2(d_3(\dot{\epsilon}_1 + \dot{\epsilon}_f) + d_4(\dot{\phi}cos\epsilon_f + \phi\dot{\epsilon}_1 sin\epsilon_f))^2 \\
& + \tfrac{1}{2}m_2 d_3^2(\dot{\phi}sin\epsilon_f - \phi\dot{\epsilon}_1 cos\epsilon_f)^2 \\
& + m_2 d_4(\dot{x}_n cos\epsilon_1 + \dot{y}_n sin\epsilon_1 + h_2\phi\dot{\epsilon}_1 - d_2\phi\dot{\epsilon}_1)(-\dot{\phi}sin\epsilon_f + \phi\dot{\epsilon}_1 cos\epsilon_f)\mathbf{i_{s1}} \cdot \mathbf{i_{s2}} \\
& - m_2(\dot{x}_n cos\epsilon_1 + \dot{y}_n sin\epsilon_1 + h_2\phi\dot{\epsilon}_1 - d_2\phi\dot{\epsilon}_1)(d_3(\dot{\epsilon}_1 + \dot{\epsilon}_f) + d_4(\dot{\phi}cos\epsilon_f + \phi\dot{\epsilon}_1 sin\epsilon_f))\mathbf{i_{s1}} \cdot \mathbf{j_{s2}} \\
& + m_2 d_4(-\dot{x}_n sin\epsilon_1 + \dot{y}_n cos\epsilon_1 - h_2\dot{\phi} - d_1\dot{\epsilon}_1 + d_2\dot{\phi})(-\dot{\phi}sin\epsilon_f + \phi\dot{\epsilon}_1 cos\epsilon_f)\mathbf{j_{s1}} \cdot \mathbf{i_{s2}}
\end{aligned}
$$

$$
\begin{aligned}
& - m_2(-\dot{x}_n sin\epsilon_1 + \dot{y}_n cos\epsilon_1 - h_2\dot{\phi} - d_1\dot{\epsilon}_1 + d_2\dot{\phi})(d_3(\dot{\epsilon}_1 + \dot{\epsilon}_f) + d_4(\dot{\phi}cos\epsilon_f + \phi\dot{\epsilon}_1 sin\epsilon_f))\mathbf{j_{s1}} \cdot \mathbf{j_{s2}} \\
& - m_2 d_3(\dot{x}_n sin\epsilon_1 - \dot{y}_n cos\epsilon_1 + d_1\dot{\epsilon}_1)\phi(\dot{\phi}sin\epsilon_f - \phi\dot{\epsilon}_1 cos\epsilon_f)\mathbf{k_{s1}} \cdot \mathbf{k_{s2}} \\
& + \tfrac{1}{2}I_{x2}(\dot{\phi}cos\epsilon_f + \phi\dot{\epsilon}_1 sin\epsilon_f)^2 + \tfrac{1}{2}I_{y2}(-\dot{\phi}sin\epsilon_f + \phi\dot{\epsilon}_1 cos\epsilon_f)^2 + \tfrac{1}{2}I_{z2}(\dot{\epsilon}_1 + \dot{\epsilon}_f)^2
\end{aligned}
\tag{40}
$$

Recall from the definition of the coordinate system that

$$\mathbf{i_{s1}} \cdot \mathbf{i_{s2}} = cos\ \epsilon_f \tag{41}$$

12

$$\mathbf{i_{s1}} \cdot \mathbf{j_{s2}} = -sin\ \epsilon_f \qquad (42)$$

$$\mathbf{j_{s1}} \cdot \mathbf{i_{s2}} = sin\ \epsilon_f \qquad (43)$$

$$\mathbf{j_{s1}} \cdot \mathbf{j_{s2}} = cos\ \epsilon_f \qquad (44)$$

and

$$\mathbf{k_{s1}} \cdot \mathbf{k_{s2}} = 1 \qquad (45)$$

Substituting Eqs. (41), (42), (43), (44) and (45) into (40), we obtain

$$
\begin{aligned}
T_2 = \quad & \tfrac{1}{2}m_2(\dot{x}_n cos\epsilon_1 + \dot{y}_n sin\epsilon_1 + h_2\phi\dot{\epsilon}_1 - d_2\phi\dot{\epsilon}_1)^2 \\
& + \tfrac{1}{2}m_2(-\dot{x}_n sin\epsilon_1 + \dot{y}_n cos\epsilon_1 - h_2\dot{\phi} - d_1\dot{\epsilon}_1 + d_2\dot{\phi})^2 \\
& + \tfrac{1}{2}m_2(\dot{x}_n sin\epsilon_1 - \dot{y}_n cos\epsilon_1 + d_1\dot{\epsilon}_1)^2\phi^2 \\
& + \tfrac{1}{2}m_2 d_4^2(-\dot{\phi}sin\epsilon_f + \phi\dot{\epsilon}_1 cos\epsilon_f)^2 \\
& + \tfrac{1}{2}m_2(d_3(\dot{\epsilon}_1 + \dot{\epsilon}_f) + d_4(\dot{\phi}cos\epsilon_f + \phi\dot{\epsilon}_1 sin\epsilon_f))^2 \\
& + \tfrac{1}{2}m_2 d_3^2(\dot{\phi}sin\epsilon_f - \phi\dot{\epsilon}_1 cos\epsilon_f)^2 \\
& + m_2 d_4 cos\epsilon_f(\dot{x}_n cos\epsilon_1 + \dot{y}_n sin\epsilon_1 + h_2\phi\dot{\epsilon}_1 - d_2\phi\dot{\epsilon}_1)(-\dot{\phi}sin\epsilon_f + \phi\dot{\epsilon}_1 cos\epsilon_f) \\
& + m_2 sin\epsilon_f(\dot{x}_n cos\epsilon_1 + \dot{y}_n sin\epsilon_1 + h_2\phi\dot{\epsilon}_1 - d_2\phi\dot{\epsilon}_1)(d_3(\dot{\epsilon}_1 + \dot{\epsilon}_f) + d_4(\dot{\phi}cos\epsilon_f + \phi\dot{\epsilon}_1 sin\epsilon_f)) \\
& + m_2 d_4 sin\epsilon_f(-\dot{x}_n sin\epsilon_1 + \dot{y}_n cos\epsilon_1 - h_2\dot{\phi} - d_1\dot{\epsilon}_1 + d_2\dot{\phi})(-\dot{\phi}sin\epsilon_f + \phi\dot{\epsilon}_1 cos\epsilon_f) \\
& - m_2 cos\epsilon_f(-\dot{x}_n sin\epsilon_1 + \dot{y}_n cos\epsilon_1 - h_2\dot{\phi} - d_1\dot{\epsilon}_1 + d_2\dot{\phi})(d_3(\dot{\epsilon}_1 + \dot{\epsilon}_f) + d_4(\dot{\phi}cos\epsilon_f + \phi\dot{\epsilon}_1 sin\epsilon_f)) \\
& - m_2 d_3(\dot{x}_n sin\epsilon_1 - \dot{y}_n cos\epsilon_1 + d_1\dot{\epsilon}_1)\phi(\dot{\phi}sin\epsilon_f - \phi\dot{\epsilon}_1 cos\epsilon_f) \\
& + \tfrac{1}{2}I_{x2}(\dot{\phi}cos\epsilon_f + \phi\dot{\epsilon}_1 sin\epsilon_f)^2 \\
& + \tfrac{1}{2}I_{y2}(-\dot{\phi}sin\epsilon_f + \phi\dot{\epsilon}_1 cos\epsilon_f)^2 \\
& + \tfrac{1}{2}I_{z2}(\dot{\epsilon}_1 + \dot{\epsilon}_f)^2
\end{aligned}
\qquad (46)
$$

Potential Energy

The change of the potential energy for the tractor of a tractor-semitrailer vehicle is primarily due to the roll motion. However, the change of potential energy for the semitrailer is affected by both the roll and pitch motion at the linking joint (fifth wheel). Furthermore, the compliance at the fifth wheel will be significant in describing the roll motion of the trailer. For simplicity, these complicated coupling will not be modeled. Instead, the roll motion is approximated as if the articulation angle is zero, that is, the truck is in straight configuration. This approximation for roll motion will be examined by comparing simulation results and experimental data in section 7. Thus the potential energy can be obtained as

$$V = m_1 g h_2(cos\phi - 1) + m_2 g((h_2 - d_2 + d_4)(cos\phi - 1)$$

13

The Lagrangian, L, is defined as

$$L = T_1 + T_2 - V \tag{47}$$

and will be used to derive vehicle body dynamics in the next section.

4   Equations of Motion

In this section a set of five second-order ordinary differential equations governing the vehicle sprung mass will be obtained in two steps. First, the vehicle sprung mass dynamics with respect to the inertial reference frame $X_n Y_n Z_n$ will be derived by utilizing Lagrange's equation. Second, since the equations of motion with respect to the unsprung mass coordinate are more meaningful, we will transform the vehicle dynamics from the inertial reference frame to the unsprung mass reference frame.

Step 1   Vehicle Body Dynamics with respect to Inertial Reference Frame

In section **3** we obtain the kinetic energy and potential energy of the tractor-semitrailer vehicle, and the Lagrangian is defined as

$$L = T_1 + T_2 - V$$

By using Lagrange's equation,

$$\frac{d}{dt}\frac{\partial L}{\partial \dot{x}_n} - \frac{\partial L}{\partial x_n} = Fg_{x_n} \tag{48}$$

we obtain the first dynamic equation

$$
\begin{aligned}
&(m_1 + m_2)(1 + \phi^2 sin^2\epsilon_1)\ddot{x}_n - (m_1 + m_2)\phi^2 sin\epsilon_1 cos\epsilon_1 \ddot{y}_n \\
&+(m_1 h_2 + m_2(h_2 - d_2 + d_4) - m_2 d_3\phi sin\epsilon_f)sin\epsilon_1\ddot{\phi} \\
&+((m_1 h_2 + m_2(h_2 - d_2 + d_4))\phi cos\epsilon_1 + m_2 d_1 sin\epsilon_1 + m_2 d_3 sin\epsilon_f cos\epsilon_1 + m_2 d_3 cos\epsilon_f sin\epsilon_1 \\
&+m_2(d_1 + d_3 cos\epsilon_f)sin\epsilon_1\phi^2)\ddot{\epsilon}_1 \\
&+m_2 d_3(sin\epsilon_1 cos\epsilon_f + cos\epsilon_1 sin\epsilon_f)\ddot{\epsilon}_f \\
&+2(m_1 + m_2)\phi sin^2\epsilon_1 \dot{x}_n\dot{\phi} + 2(m_1 + m_2)\phi^2 sin\epsilon_1 cos\epsilon_1 \dot{x}_n\dot{\epsilon}_1 - 2(m_1 + m_2)\phi sin\epsilon_1 cos\epsilon_1 \dot{y}_n\dot{\phi} \\
&-(m_1 + m_2)\phi^2(cos^2\epsilon_1 - sin^2\epsilon_1)\dot{y}_n\dot{\epsilon}_1 + (2m_1 h_2 + 2m_2(h_2 - d_2 + d_4) - m_2 d_3\phi sin\epsilon_f)cos\epsilon_1\dot{\phi}\dot{\epsilon}_1 \\
&-m_2 d_3 sin\epsilon_1 sin\epsilon_f \dot{\phi}^2 + 2(m_2 d_1 sin\epsilon_1 + m_2 d_3 sin\epsilon_1 cos\epsilon_f)\dot{\phi}\dot{\epsilon}_1 - m_2 d_3\phi sin\epsilon_1 cos\epsilon_f \dot{\phi}\dot{\epsilon}_f \\
&-(m_1 h_2 + m_2(h_2 - d_2 + d_4))\phi sin\epsilon_1\dot{\epsilon}_1^2 + m_2 d_1 cos\epsilon_1\dot{\epsilon}_1^2 + m_2 d_3(cos\epsilon_1 cos\epsilon_f - sin\epsilon_1 sin\epsilon_f)\dot{\epsilon}_1^2 \\
&+m_2(d_1 + d_3 cos\epsilon_f)cos\epsilon_1\phi^2\dot{\epsilon}_1^2 + 2m_2 d_3(cos\epsilon_1 cos\epsilon_f - sin\epsilon_1 sin\epsilon_f)\dot{\epsilon}_1\dot{\epsilon}_f \\
&-m_2 d_3 sin\epsilon_1 sin\epsilon_f \phi^2\dot{\epsilon}_1\dot{\epsilon}_f + m_2 d_3(cos\epsilon_1 cos\epsilon_f - sin\epsilon_1 sin\epsilon_f)\dot{\epsilon}_f^2 = Fg_{x_n}
\end{aligned}
\tag{49}
$$

where Fg,, is the generalized force corresponding to the generalized coordinate x_n. By using Lagrange's equation

$$\frac{d}{dt}\frac{\partial L}{\partial \dot{y}_n} - \frac{\partial L}{\partial y_n} = Fg_{y_n} \tag{50}$$

we obtain the second dynamic equation

$$
\begin{aligned}
&-(m_1 + m_2)\phi^2 sin\epsilon_1 cos\epsilon_1 \ddot{x}_n + (m_1 + m_2)(1 + \phi^2 cos^2\epsilon_1)\ddot{y}_n \\
&-(m_1 h_2 + m_2(h_2 - d_2 + d_4) - m_2 d_3 \phi sin\epsilon_f)cos\epsilon_1 \ddot{\phi} \\
&+((m_1 h_2 + m_2(h_2 - d_2 + d_4))\phi sin\epsilon_1 - m_2(d_1 + d_3 cos\epsilon_f)cos\epsilon_1 + m_2 d_3 sin\epsilon_f sin\epsilon_1 \\
&-m_2(d_1 + d_3 cos\epsilon_f)cos\epsilon_1 \phi^2)\ddot{\epsilon}_1 \\
&+m_2 d_3(sin\epsilon_1 sin\epsilon_f - cos\epsilon_1 cos\epsilon_f)\ddot{\epsilon}_f \\
&-2(m_1 + m_2)\phi sin\epsilon_1 cos\epsilon_1 \dot{x}_n \dot{\phi} - (m_1 + m_2)\phi^2(cos^2\epsilon_1 - sin^2\epsilon_1)\dot{x}_n \dot{\epsilon}_1 + 2(m_1 + m_2)\phi cos^2\epsilon_1 \dot{y}_n \dot{\phi} \\
&-2(m_1 + m_2)\phi^2 sin\epsilon_1 cos\epsilon_1 \dot{y}_n \dot{\epsilon}_1 + m_2 d_3 sin\epsilon_f cos\epsilon_1 \dot{\phi}^2 \\
&+(2m_1 h_2 + 2m_2(h_2 - d_2 + d_4) - m_2 d_3 \phi sin\epsilon_f)sin\epsilon_1 \dot{\phi}\dot{\epsilon}_1 - 2m_2(d_1 + d_3 cos\epsilon_f)cos\epsilon_1 \dot{\phi}\dot{\epsilon}_1 \\
&+m_2 d_3 \phi cos\epsilon_1 cos\epsilon_f \dot{\phi}\dot{\epsilon}_f + (m_1 h_2 + m_2(h_2 - d_2 + d_4))\phi cos\epsilon_1 \dot{\epsilon}_1^2 + m_2 d_1 sin\epsilon_1 \dot{\epsilon}_1^2 \\
&+m_2 d_3(sin\epsilon_1 cos\epsilon_f + cos\epsilon_1 sin\epsilon_f)\dot{\epsilon}_1^2 + m_2(d_1 + d_3 cos\epsilon_f)\phi^2 sin\epsilon_1 \dot{\epsilon}_1^2 \\
&+2m_2 d_3(cos\epsilon_1 sin\epsilon_f + sin\epsilon_1 cos\epsilon_f)\dot{\epsilon}_1 \dot{\epsilon}_f + m_2 d_3 cos\epsilon_1 sin\epsilon_f \phi^2 \dot{\epsilon}_1 \dot{\epsilon}_f \\
&+m_2 d_3(sin\epsilon_1 cos\epsilon_f + cos\epsilon_1 sin\epsilon_f)\dot{\epsilon}_f^2 = Fg_{y_n}
\end{aligned}
\tag{51}
$$

where Fg_{y_n} is the generalized force corresponding to the generalized coordinate y_n. We proceed by using Lagrange's equation

$$\frac{d}{dt}\frac{\partial L}{\partial \dot{\phi}} - \frac{\partial L}{\partial \phi} = Fg_{\phi} \tag{52}$$

to obtain the third dynamic equation

$$
\begin{aligned}
&(m_1 h_2 + m_2(h_2 - d_2 + d_4) - m_2 d_3 \phi sin\epsilon_f)sin\epsilon_1 \ddot{x}_n \\
&-(m_1 h_2 + m_2(h_2 - d_2 + d_4) - m_2 d_3 \phi sin\epsilon_f)cos\epsilon_1 \ddot{y}_n \\
&(I_{x1} + m_1 h_2^2 + I_{x2}cos^2\epsilon_f + m_2(h_2 - d_2 + d_4)^2 + (I_{y2} + m_2 d_3^2)sin^2\epsilon_f)\ddot{\phi} \\
&(m_2(d_1 + d_3 cos\epsilon_f)(h_2 - d_2 + d_4) + (I_{x2} - I_{y2} - m_2 d_3^2)\phi sin\epsilon_f cos\epsilon_f - m_2 d_1 d_3 \phi sin\epsilon_f)\ddot{\epsilon}_1 \\
&+m_2 d_3(h_2 - d_2 + d_4)cos\epsilon_f \ddot{\epsilon}_f \\
&-2m_2 d_3 sin\epsilon_1 sin\epsilon_f \dot{x}_n \dot{\phi} - m_2 d_3 \phi(cos\epsilon_1 sin\epsilon_f + 2sin\epsilon_1 cos\epsilon_f)\dot{x}_n \dot{\epsilon}_1 - m_2 d_3 \phi sin\epsilon_1 cos\epsilon_f \dot{x}_n \dot{\epsilon}_f \\
&+2m_2 d_3 cos\epsilon_1 sin\epsilon_f \dot{y}_n \dot{\phi} + m_2 d_3 \phi(-sin\epsilon_1 sin\epsilon_f + 2cos\epsilon_1 cos\epsilon_f)\dot{y}_n \dot{\epsilon}_1 + m_2 d_3 \phi cos\epsilon_1 cos\epsilon_f \dot{y}_n \dot{\epsilon}_f \\
&+2(I_{y2} + m_2 d_3^2 - I_{x2})sin\epsilon_f cos\epsilon_f \dot{\phi}\dot{\epsilon}_f \\
&+((I_{x2} - I_{y2} - m_2 d_3^2)\phi(cos^2\epsilon_f - sin^2\epsilon_f) - m_2 d_1 d_3 \phi cos\epsilon_f - 2m_2 d_3(h_2 - d_2 + d_4)sin\epsilon_f)\dot{\epsilon}_1 \dot{\epsilon}_f \\
&-m_2 d_3(h_2 - d_2 + d_4)sin\epsilon_f \dot{\epsilon}_f^2 \\
&-(I_{y1} + m_1 h_2^2 + I_{x2}sin^2\epsilon_f + (I_{y2} + m_2 d_3^2)cos^2\epsilon_f + m_2 d_1^2 + m_2(h_2 - d_2 + d_4)^2 + 2m_2 d_1 d_3 cos\epsilon_f)\phi \dot{\epsilon}_1^2 \\
&-(m_1 + m_2)\phi(\dot{x}_n sin\epsilon_1 - \dot{y}_n cos\epsilon_1)^2 - 2m_2 d_1 \phi \dot{\epsilon}_1(\dot{x}_n sin\epsilon_1 - \dot{y}_n cos\epsilon_1) \\
&-m_2 d_3(h_2 - d_2 + d_4)sin\epsilon_f \dot{\epsilon}_1^2 = Fg_{\phi}
\end{aligned}
\tag{53}
$$

where Fg_{ϕ} is the generalized force corresponding to the generalized coordinate ϕ. From Lagrange's equation

$$\frac{d}{dt}\frac{\partial L}{\partial \dot{\epsilon}_1} - \frac{\partial L}{\partial \epsilon_1} = Fg_{\epsilon_1} \tag{54}$$

15

the fourth equation is obtained as

$$
\begin{aligned}
&(m_1 h_2 \phi cos\epsilon_1 + m_2(h_2 - d_2 + d_4)\phi cos\epsilon_1 + m_2 d_3(sin\epsilon_1 cos\epsilon_f + cos\epsilon_1 sin\epsilon_f) \\
&+ m_2 d_1 sin\epsilon_1 + m_2(d_1 + d_3 cos\epsilon_f)\phi^2 sin\epsilon_1)\ddot{x}_n \\
&(m_1 h_2 \phi sin\epsilon_1 + m_2(h_2 - d_2 + d_4)\phi sin\epsilon_1 - m_2 d_3(cos\epsilon_1 cos\epsilon_f - sin\epsilon_1 sin\epsilon_f) \\
&- m_2 d_1 cos\epsilon_1 - m_2(d_1 + d_3 cos\epsilon_f)\phi^2 cos\epsilon_1)\ddot{y}_n \\
&(m_2(d_1 + d_3 cos\epsilon_f)(h_2 - d_2 + d_4) - m_2 d_1 d_3 \phi sin\epsilon_f + (I_{x2} - I_{y2} - m_2 d_3^2)\phi sin\epsilon_f cos\epsilon_f)\ddot{\phi} \\
&(I_{z1} + I_{z2} + m_2(d_1 + d_3 cos\epsilon_f)^2 + m_2(d_3 sin\epsilon_f + (h_2 - d_2 + d_4)\phi)^2 \\
&+ (I_{y1} + m_1 h_2^2 + m_2(d_1 + d_3 cos\epsilon_f)^2 + I_{x2}sin^2\epsilon_f + I_{y2}cos^2\epsilon_f)\phi^2)\ddot{\epsilon}_1 \\
&(I_{z2} + m_2 d_3^2 + m_2 d_1 d_3 cos\epsilon_f + m_2 d_3(h_2 - d_2 + d_4)\phi sin\epsilon_f)\ddot{\epsilon}_f \\
&+ 2m_2(d_1 + d_3 cos\epsilon_f)\phi\dot{\phi}(\dot{x}_n sin\epsilon_1 - \dot{y}_n cos\epsilon_1) - m_2 d_3 \phi^2 sin\epsilon_f \dot{\epsilon}_f(\dot{x}_n sin\epsilon_1 - \dot{y}_n cos\epsilon_1) \\
&- (m_1 + m_2)\phi^2(\dot{x}_n cos\epsilon_1 + \dot{y}_n sin\epsilon_1)(\dot{x}_n sin\epsilon_1 - \dot{y}_n cos\epsilon_1) + m_2 d_3 \phi sin\epsilon_f \dot{\phi}(\dot{x}_n cos\epsilon_1 + \dot{y}_n sin\epsilon_1) \\
&+ ((I_{x2} - I_{y2} - m_2 d_3^2)sin\epsilon_f cos\epsilon_f - m_2 d_1 d_3 sin\epsilon_f)\dot{\phi}^2 + 2m_2 d_3(h_2 - d_2 + d_4)sin\epsilon_f \dot{\phi}\dot{\epsilon}_1 \\
&+ 2(I_{y1} + m_1 h_2^2 + m_2(d_1 + d_3 cos\epsilon_f)^2 + I_{x2}sin^2\epsilon_f + I_{y2}cos^2\epsilon_f)\phi\dot{\phi}\dot{\epsilon}_1 \\
&- (m_2 d_1 d_3 cos\epsilon_f + (I_{x2} - I_{y2} - m_2 d_3^2)(sin^2\epsilon_f - cos^2\epsilon_f))\phi\dot{\phi}\dot{\epsilon}_f \\
&+ (-2m_2 d_3 sin\epsilon_f(d_1 + d_3 cos\epsilon_f)(1 + \phi^2) + 2m_2 d_3 cos\epsilon_f(d_3 sin\epsilon_f + (h_2 - d_2 + d_4)\phi) \\
&+ 2(I_{x2} - I_{y2})sin\epsilon_f cos\epsilon_f \phi^2)\dot{\epsilon}_1 \dot{\epsilon}_f \\
&(m_2 d_3(h_2 - d_2 + d_4)\phi cos\epsilon_f - m_2 d_1 d_3 sin\epsilon_f)\dot{\epsilon}_f^2 = Fg_{\epsilon_1}
\end{aligned}
\tag{55}
$$

where Fg_{ϵ_1} is the generalized force corresponding to the generalized coordinate ϵ_1. The last dynamic equation is obtained by using Lagrange's equation

$$
\frac{d}{dt}\frac{\partial L}{\partial \dot{\epsilon}_f} - \frac{\partial L}{\partial \epsilon_f} = Fg_{\epsilon_f}
\tag{56}
$$

Thus we have

$$
\begin{aligned}
&m_2 d_3(sin\epsilon_1 cos\epsilon_f + cos\epsilon_1 sin\epsilon_f)\ddot{x}_n \\
&- m_2 d_3(cos\epsilon_1 cos\epsilon_f - sin\epsilon_1 sin\epsilon_f)\ddot{y}_n \\
&+ m_2 d_3(h_2 - d_2 + d_4)cos\epsilon_f \ddot{\phi} \\
&+ (I_{z2} + m_2 d_3^2 + m_2 d_1 d_3 cos\epsilon_f + m_2 d_3(h_2 - d_2 + d_4)\phi sin\epsilon_f)\ddot{\epsilon}_1 \\
&+ (I_{z2} + m_2 d_3^2)\ddot{\epsilon}_f \\
&+ 2m_2 d_3(h_2 - d_2 + d_4)sin\epsilon_f \dot{\phi}\dot{\epsilon}_1 - m_2 d_3(h_2 - d_2 + d_4)\phi cos\epsilon_f \dot{\epsilon}_1^2 + m_2 d_1 d_3 sin\epsilon_f \dot{\epsilon}_1^2 \\
&+ 2m_2 d_4 sin\epsilon_f cos\epsilon_f \dot{\phi}(\dot{x}_n sin\epsilon_1 - \dot{y}_n cos\epsilon_1 + (h_2 - d_2)\dot{\phi} + d_1 \dot{\epsilon}_1) \\
&+ m_2 d_3 \phi cos\epsilon_f \dot{\phi}(\dot{x}_n sin\epsilon_1 - \dot{y}_n cos\epsilon_1 + d_1 \dot{\epsilon}_1) + m_2 d_3 \phi^2 sin\epsilon_f \dot{\epsilon}_1(\dot{x}_n sin\epsilon_1 - \dot{y}_n cos\epsilon_1 + d_1 \dot{\epsilon}_1) \\
&+ (I_{x2} - I_{y2} - m_2 d_3^2)sin\epsilon_f cos\epsilon_f \dot{\phi}^2 + (I_{x2} - I_{y2} - m_2 d_3^2)(sin^2\epsilon_f - cos^2\epsilon_f)\phi\dot{\phi}\dot{\epsilon}_1 \\
&- (I_{x2} - I_{y2} - m_2 d_3^2)sin\epsilon_f cos\epsilon_f \phi^2 \dot{\epsilon}_1^2 = Fg_{\epsilon_f}
\end{aligned}
\tag{57}
$$

where Fg_{ϵ_f} is the generalized force corresponding to the generalized coordinate ϵ_f.

Eqs. (49), (51), (53), (55) and (57) describe the dynamic behavior of the tractor-semitrailer vehicle seen from the inertial reference frame $X_n Y_n Z_n$.

Step 2   Vehicle Body Dynamics with respect to the Unsprung Mass Reference Frame

In this step, the vehicle model will be transformed from the inertial reference frame to the unsprung mass reference frame. Recall in section 2 that the transformations can be conducted by using

$$
\dot{x}_n \cos \epsilon_1 + \dot{y}_n \sin \epsilon_1 = x_r
\tag{58}
$$

16

$$-\dot{x}_n \, \sin \, \epsilon_1 + \dot{y}_n \, \cos \, \epsilon_1 = \dot{y}_u \tag{59}$$

$$\ddot{x}_n \cos \, \epsilon_1 + \ddot{y}_n \sin \, \epsilon_1 = \ddot{x}_u - \dot{y}_u \dot{\epsilon}_1 \tag{60}$$

and

$$-\ddot{x}_n \sin \, \epsilon_1 + \ddot{y}_n \cos \, \epsilon_1 = \ddot{y}_u + \dot{x}_u \dot{\epsilon}_1, \tag{61}$$

where $\dot{x}_n$ is the vehicle velocity component along the X_n axis of the inertial reference frame, $\dot{y}_n$ is the vehicle velocity component along the Y_n axis of the inertial reference frame, $\dot{x}_u$ is the vehicle velocity component along the X_u axis of the unsprung mass reference frame, and $\dot{y}_u$ is the vehicle velocity component along the Y_u axis of the unsprung mass reference frame.

By adding the first dynamic equation in the inertial reference frame (49) $\times$ $cos\epsilon_1$ and the second dynamic equation (51) $\times$ $sin\epsilon_1$ and using (58), (59), (60), and (61), we obtain the first dynamic equation in the unsprung mass reference frame as

$$
\begin{aligned}
&(m_1 + m_2)\ddot{x}_u + (m_1 h_2 \phi + m_2(h_2 - d_2 + d_4)\phi + m_2 d_3 sin\epsilon_f)\ddot{\epsilon}_1 + m_2 d_3 sin\epsilon_f \ddot{\epsilon}_f \\
&-(m_1 + m_2)(1 + \phi^2)\dot{y}_u \dot{\epsilon}_1 + (2m_1 h_2 + 2m_2(h_2 - d_2 + d_4) - m_2 d_3 \phi sin\epsilon_f)\dot{\phi}\dot{\epsilon}_1 \\
&+m_2(d_1 + d_3 cos\epsilon_f)(1 + \phi^2)\dot{\epsilon}_1^2 + 2m_2 d_3 cos\epsilon_f \dot{\epsilon}_1 \dot{\epsilon}_f + m_2 d_3 cos\epsilon_f \dot{\epsilon}_f^2 \\
&= Fg_{x_n} \times cos\epsilon_1 + Fg_{y_n} \times sin\epsilon_1
\end{aligned}
\tag{62}
$$

Similarly, by subtracting Eq. (49) $\times$ $sin\epsilon_1$ from Eq. (51) $\times$ $cos\epsilon_1$ and using (58), (59), (60) and (61), we obtain the second dynamic equation in the unsprung mass reference frame as

$$
\begin{aligned}
&(m_1 + m_2)(1 + \phi^2)\ddot{y}_u - (m_1 h_2 + m_2(h_2 - d_2 + d_4) - m_2 d_3 \phi sin\epsilon_f)\ddot{\phi} \\
&-m_2(d_1 + d_3 cos\epsilon_f)(1 + \phi^2)\ddot{\epsilon}_1 - m_2 d_3 cos\epsilon_f \ddot{\epsilon}_f \\
&(m_1 + m_2)\dot{x}_u \dot{\epsilon}_1 + 2(m_1 + m_2)\phi \dot{y}_u \dot{\phi} + m_2 d_3 sin\epsilon_f \dot{\phi}^2 - 2m_2(d_1 + d_3 cos\epsilon_f)\phi \dot{\phi}\dot{\epsilon}_1 \\
&+m_2 d_3 \phi cos\epsilon_f \dot{\phi}\dot{\epsilon}_f + (m_1 h_2 + m_2(h_2 - d_2 + d_4))\dot{\phi}\dot{\epsilon}_1^2 + m_2 d_3 sin\epsilon_f \dot{\epsilon}_1^2 \\
&+2m_2 d_3 sin\epsilon_f \dot{\epsilon}_1 \dot{\epsilon}_f + m_2 d_3 sin\epsilon_f \phi^2 \dot{\epsilon}_1 \dot{\epsilon}_f + m_2 d_3 sin\epsilon_f \dot{\epsilon}_f^2 \\
&= -Fg_{x_n} \times sin\epsilon_1 + Fg_{y_n} \times cos\epsilon_1
\end{aligned}
\tag{63}
$$

By substituting (58), (59), (60) and (61) into the third dynamic equation (53) in the inertial reference frame, the third dynamic equation in the unsprung mass reference frame can be obtained as

$$
\begin{aligned}
&-(m_1 h_2 + m_2(h_2 - d_2 + d_4) - m_2 d_3 \phi sin\epsilon_f)\ddot{y}_u \\
&(I_{x1} + m_1 h_2^2 + I_{x2}cos^2\epsilon_f + m_2(h_2 - d_2 + d_4)^2 + (I_{y2} + m_2 d_3^2)sin^2\epsilon_f)\ddot{\phi} \\
&(m_2(d_1 + d_3 cos\epsilon_f)(h_2 - d_2 + d_4) + (I_{x2} - I_{y2} - m_2 d_3^2)\phi sin\epsilon_f cos\epsilon_f - m_2 d_1 d_3 \phi sin\epsilon_f)\ddot{\epsilon}_1 \\
&+m_2 d_3(h_2 - d_2 + d_4)cos\epsilon_f \ddot{\epsilon}_f \\
&-(m_1 h_2 + m_2(h_2 - d_2 + d_4))\dot{x}_u \dot{\epsilon}_1 + 2m_2 d_3 \phi cos\epsilon_f \dot{y}_u \dot{\epsilon}_1 + m_2 d_3 \phi cos\epsilon_f \dot{y}_u \dot{\epsilon}_f \\
&+2m_2 d_3 sin\epsilon_f \dot{y}_u \dot{\phi} + 2(I_{y2} + m_2 d_3^2 - I_{x2})sin\epsilon_f cos\epsilon_f \dot{\phi}\dot{\epsilon}_f \\
&-(2m_2 d_3(h_2 - d_2 + d_4)sin\epsilon_f + m_2 d_1 d_3 \phi cos\epsilon_f)\dot{\epsilon}_1 \dot{\epsilon}_f \\
&-(I_{x2} - I_{y2} - m_2 d_3^2)\phi(sin^2 \epsilon_f - cos^2 \epsilon_f)\dot{\epsilon}_1 \dot{\epsilon}_f - m_2 d_3(h_2 - d_2 + d_4)sin\epsilon_f \dot{\epsilon}_f^2 \\
&-(m_1 h_2^2 + I_{y1} + m_2(h_2 - d_2 + d_4)^2 + I_{x2}sin^2\epsilon_f + (I_{y2} + m_2 d_3^2)cos^2\epsilon_f)\phi \dot{\epsilon}_1^2 \\
&+(m_2 d_1^2 + 2m_2 d_1 d_3 cos\epsilon_f)\phi \dot{\epsilon}_1^2 - (m_1 + m_2)\phi \dot{y}_u^2 + 2m_2 d_1 \phi \dot{y}_u \dot{\epsilon}_1 \\
&-m_2 d_3(h_2 - d_2 + d_4)sin\epsilon_f \dot{\epsilon}_1^2 = Fg_\phi
\end{aligned}
\tag{64}
$$

17

The fourth and fifth dynamic equations can also be obtained from (55) and (57) as

$$
\begin{aligned}
&(m_1h_2\phi + m_2(h_2 - d_2 + d_4)\phi + m_2d_3sin\epsilon_f)\ddot{x}_u \\
&-m_2(d_1 + d_3cos\epsilon_f)(1 + \phi^2)\ddot{y}_u \\
&(m_2(d_1 + d_3cos\epsilon_f)(h_2 - d_2 + d_4) + (I_{x2} - I_{y2} - m_2d_3^2)\phi sin\epsilon_f cos\epsilon_f - m_2d_1d_3\phi sin\epsilon_f)\ddot{\phi} \\
&(I_{z1} + I_{z2} + m_2(d_1 + d_3cos\epsilon_f)^2 + m_2(d_3sin\epsilon_f + (h_2 - d_2 + d_4)\phi)^2 \\
&+(I_{y1} + m_1h_2^2 + m_2(d_1 + d_3cos\epsilon_f)^2 + I_{x2}sin^2\epsilon_f + I_{y2}cos^2\epsilon_f)\phi^2)\ddot{\epsilon}_1 \\
&(I_{z2} + m_2d_3^2 + m_2d_1d_3cos\epsilon_f + m_2d_3(h_2 - d_2 + d_4)\phi sin\epsilon_f)\ddot{\epsilon}_f \\
&-(m_2d_1 + m_2d_3cos\epsilon_f)(1 + \phi^2)\dot{x}_u\dot{\epsilon}_1 - (m_1h_2 + m_2(h_2 - d_2 + d_4))\phi\dot{y}_u\dot{\epsilon}_1 - m_2d_3sin\epsilon_f\dot{y}_u\dot{\epsilon}_1 \\
&-2(m_2d_1 + m_2d_3cos\epsilon_f)\phi\dot{y}_u\dot{\phi} + m_2d_3\phi^2sin\epsilon_f\dot{y}_u\dot{\epsilon}_f + (m_1 + m_2)\phi^2\dot{x}_u\dot{y}_u \\
&+m_2d_3\phi sin\epsilon_f\dot{x}_u\dot{\phi} + ((I_{x2} - I_{y2} - m_2d_3^2)sin\epsilon_f cos\,\epsilon_f - m_2d_1d_3sin\epsilon_f)\dot{\phi}^2 \\
&+2m_2(h_2 - d_2 + d_4)(d_3sin\epsilon_f + (h_2 - d_2 + d_4)\phi)\dot{\phi}\dot{\epsilon}_1 \\
&+2(m_1h_2^2 + I_{y1} + m_2(d_1 + d_3cos\epsilon_f)(d_1 + d_3cos\epsilon_f) + I_{x2}sin^2\epsilon_f + I_{y2}cos^2\epsilon_f)\phi\dot{\phi}\dot{\epsilon}_1 \\
&-(m_2d_1d_3cos\epsilon_f + (I_{x2} - I_{y2} - m_2d_3^2)(sin^2\,\epsilon_f - cos^2\,\epsilon_f))\phi\dot{\phi}\dot{\epsilon}_f \\
&+(-2m_2d_3sin\epsilon_f(d_1 + d_3cos\epsilon_f) + 2m_2d_3cos\epsilon_f(d_3sin\epsilon_f + (h_2 - d_2 + d_4)\phi))\dot{\epsilon}_1\dot{\epsilon}_f \\
&+(-2m_2d_3sin\epsilon_f(d_1 + d_3cos\epsilon_f)\phi^2 + 2(I_{x2} - I_{y2})sin\epsilon_f cos\,\epsilon_f\phi^2)\dot{\epsilon}_1\dot{\epsilon}_f \\
&+m_2d_3((h_2 - d_2 + d_4)\phi cos\epsilon_f - d_1sin\epsilon_f)\dot{\epsilon}_f^2 = Fg_{\epsilon_1},
\end{aligned}
\tag{65}
$$

and

$$
\begin{aligned}
&m_2d_3sin\epsilon_f\ddot{x}_n - m_2d_3cos\epsilon_f\ddot{y}_n + m_2d_3(h_2 - d_2 + d_4)cos\epsilon_f\ddot{\phi} \\
&(I_{z2} + m_2d_3^2 + m_2d_1d_3cos\epsilon_f + m_2d_3(h_2 - d_2 + d_4)\phi sin\epsilon_f)\ddot{\epsilon}_1 \\
&(I_{z2} + m_2d_3^2)\ddot{\epsilon}_f \\
&-m_2d_3cos\epsilon_f\dot{x}_u\dot{\epsilon}_1 - m_2d_3sin\epsilon_f\dot{y}_u\dot{\epsilon}_1 + 2m_2d_3(h_2 - d_2 + d_4)sin\epsilon_f\dot{\phi}\dot{\epsilon}_1 \\
&-m_2d_3(h_2 - d_2 + d_4)\phi cos\epsilon_f\dot{\epsilon}_1^2 + m_2d_1d_3sin\epsilon_f\dot{\epsilon}_1^2 + 2m_2d_4sin\epsilon_f cos\,\epsilon_f\dot{\phi}(-\dot{y}_u + (h_2 - d_2)\dot{\phi} + d_1\dot{\epsilon}_1) \\
&+m_2d_3\phi cos\epsilon_f\dot{\phi}(-\dot{y}_u + d_1\dot{\epsilon}_1) + m_2d_3\phi^2sin\epsilon_f\dot{\epsilon}_1(-\dot{y}_u + d_1\dot{\epsilon}_1) \\
&+(I_{x2} - I_{y2} - m_2d_3^2)sin\epsilon_f cos\,\epsilon_f\dot{\phi}^2 + (I_{x2} - I_{y2} - m_2d_3^2)(sin^2\,\epsilon_f - cos^2\,\epsilon_f)\phi\dot{\phi}\dot{\epsilon}_1 \\
&+(I_{y2} + m_2d_3^2 - I_{x2})\phi^2sin\epsilon_f cos\,\epsilon_f\dot{\epsilon}_1^2 = Fg_{\epsilon_f},
\end{aligned}
\tag{66}
$$

respectively. Eqs. (62), (63), (64), (65) and (66) constitute the first major component of the complex model for the tractor-semitrailer vehicle. The generalized forces on the right hand side of (62), (63), (64), (65) and (66) are the other major component of the complex model and will be explored in the next two sections.

5   Generalized Forces

We have seen in the previous section that deriving the generalized forces is an important part of the modeling. In this and the next sections, we will show how to obtain generalized forces, which appear on the right hand side of the dynamic equations (62), (63), (64), (65) and (66). We notice that the external forces acting on the vehicle body are from the tire/road interface and suspensions. Thus to calculate the generalized forces, we will derive the expressions for the generalized forces in terms of the longitudinal and lateral components of tire forces and the vertical suspension forces. The process of calculating generalized forces are derived from the principle of virtual work. Interested readers are refererred to (Greenwood

18

1977, Rosenberg 1977). In the next section, we will show how to obtain the longitudinal and lateral components of tire forces from the tire model and suspension forces from the suspension model. To derive the expressions of generalized forces in terms of the tire forces and suspension forces, we define the sign conventions, shown in Fig. 5, of tire forces, where F_{ai} is the longitudinal tire force and F_{bi} is the lateral tire force. The suspension force at the $i - th$ tire is denoted as F_{pi}, whose direction is perpendicular to both F_{ai} and F_{bi}.
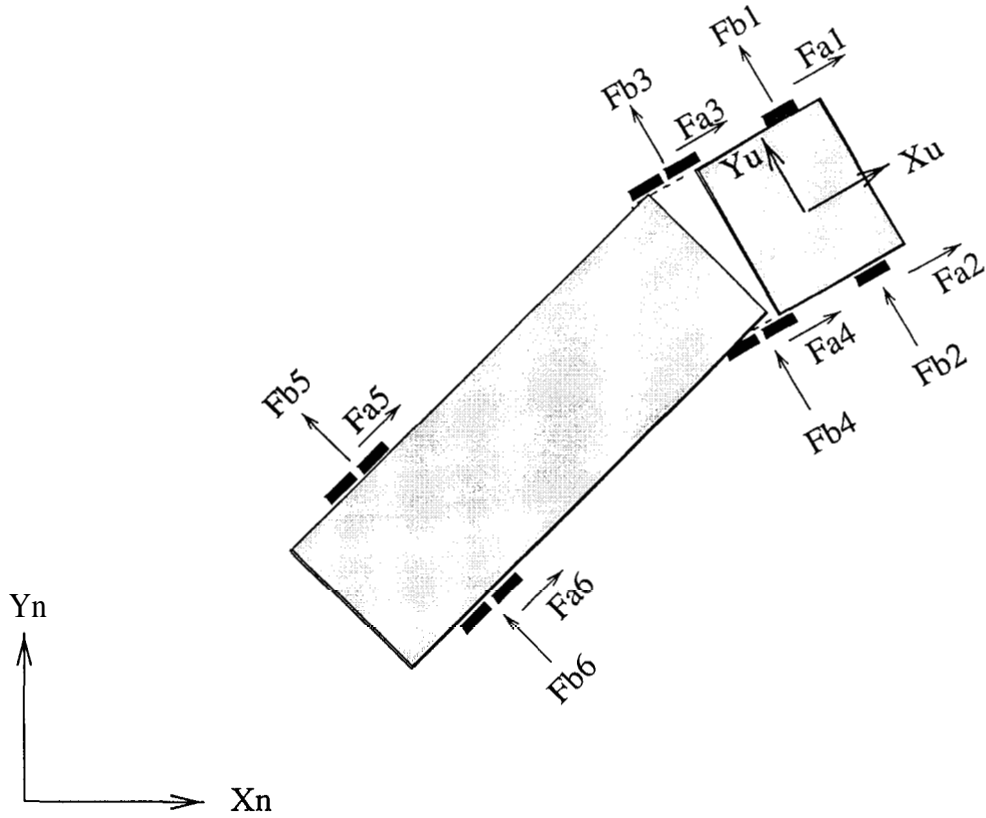
Figure 5: Definition of Tire Force in the Cartesian Coordinate

From Fig. 5, the component of the tire force along the X, axis is

$$F_{xni} = F_{ai} \cdot cos\epsilon_1 - F_{bi}sin\epsilon_1 \qquad (67)$$

for $i = 1, \cdots, 4$, and is

$$F_{xni} = F_{ai} \cdot cos(\epsilon_1 + \epsilon_f) - F_{bi}sin(\epsilon_1 + \epsilon_f) \qquad (68)$$

for $i = 5, 6$. Similarly, the component of the tire force along the Y_n axis is

$$F_{yni} = F_{ai} \cdot sin\epsilon_1 + F_{bi}cos\epsilon_1 \qquad (69)$$

19

for $i = 1, \cdots, 4$, and is

$$F_{yni} = F_{ai} \cdot sin(\epsilon_1 + \epsilon_f) + F_{bi} cos(\epsilon_1 + \epsilon_f) \tag{70}$$

for $i = 5, 6$. The position vector of the location, where the external forces F_{xn1}, F_{yn1} and F_{p1} are acting, can be obtained as

$$
\begin{aligned}
\mathbf{r_{t1}} =\ & \mathbf{r_{CG1}} + l_1 \mathbf{i_{s1}} + \frac{T_{w1}}{2} \mathbf{j_{s1}} - z_0 \mathbf{k_{s1}} \\
=\ & x_n \mathbf{i_n} + y_n \mathbf{j_n} + z_0 \mathbf{k_n} + l_1 \mathbf{i_{s1}} + \frac{T_{w1}}{2} \mathbf{j_{s1}} - z_0 \mathbf{k_{s1}}
\end{aligned}
\tag{71}
$$

By substituting the transformation matrices in section 2, we obtain the position vector $\mathbf{r_{t1}}$ in the inertial reference coordinate,

$$
\begin{aligned}
\mathbf{r_{t1}} =\ & (x_n + l_1 cos\epsilon_1 - (\tfrac{T_{w1}}{2} cos\phi + z_0 sin\phi) sin\epsilon_1) \mathbf{i_n} \\
& + (y_n + l_1 sin\epsilon_1 + (\tfrac{T_{w1}}{2} cos\phi + z_0 sin\phi) cos\epsilon_1) \mathbf{j_n} \\
& + (z_0 + \tfrac{T_{w1}}{2} sin\phi - z_0 cos\phi) \mathbf{k_n} \\
\equiv\ & r_{x_{t1}} \mathbf{i_n} + r_{y_{t1}} \mathbf{j_n} + r_{z_{t1}} \mathbf{k_n}.
\end{aligned}
\tag{72}
$$

Locations of other tire and suspension forces can be similarly obtained as

$$
\begin{aligned}
\mathbf{r_{t2}} =\ & \mathbf{r_{CG1}} + l_1 \mathbf{i_{s1}} - \frac{T_{w1}}{2} \mathbf{j_{s1}} - z_0 \mathbf{k_{s1}} \\
=\ & x_n \mathbf{i_n} + y_n \mathbf{j_n} + z_0 \mathbf{k_n} + l_1 \mathbf{i_{s1}} - \frac{T_{w1}}{2} \mathbf{j_{s1}} - z_0 \mathbf{k_{s1}} \\
=\ & (x_n + l_1 cos\epsilon_1 + (\tfrac{T_{w1}}{2} cos\phi - z_0 sin\phi) sin\epsilon_1) \mathbf{i_n} \\
& + (y_n + l_1 sin\epsilon_1 - (\tfrac{T_{w1}}{2} cos\phi - z_0 sin\phi) cos\epsilon_1) \mathbf{j_n} \\
& + (z_0 - \tfrac{T_{w1}}{2} sin\phi - z_0 cos\phi) \mathbf{k_n} \\
\equiv\ & r_{x_{t2}} \mathbf{i_n} + r_{y_{t2}} \mathbf{j_n} + r_{z_{t2}} \mathbf{k_n},
\end{aligned}
\tag{73}
$$

$$
\begin{aligned}
\mathbf{r_{t3}} =\ & \mathbf{r_{CG1}} - l_2 \mathbf{i_{s1}} + \frac{T_{w2}}{2} \mathbf{j_{s1}} - z_0 \mathbf{k_{s1}} \\
=\ & x_n \mathbf{i_n} + y_n \mathbf{j_n} + z_0 \mathbf{k_n} - l_2 \mathbf{i_{s1}} + \frac{T_{w2}}{2} \mathbf{j_{s1}} - z_0 \mathbf{k_{s1}} \\
=\ & (x_n - l_2 cos\epsilon_1 - (\tfrac{T_{w2}}{2} cos\phi + z_0 sin\phi) sin\epsilon_1) \mathbf{i_n} \\
& + (y_n - l_2 sin\epsilon_1 + (\tfrac{T_{w2}}{2} cos\phi + z_0 sin\phi) cos\epsilon_1) \mathbf{j_n} \\
& + (z_0 + \tfrac{T_{w2}}{2} sin\phi - z_0 cos\phi) \mathbf{k_n} \\
\equiv\ & r_{x_{t3}} \mathbf{i_n} + r_{y_{t3}} \mathbf{j_n} + r_{z_{t3}} \mathbf{k_n},
\end{aligned}
\tag{74}
$$

$$
\begin{aligned}
\mathbf{r_{t4}} =\ & \mathbf{r_{CG1}} - l_2 \mathbf{i_{s1}} - \frac{T_{w2}}{2} \mathbf{j_{s1}} - z_0 \mathbf{k_{s1}} \\
=\ & x_n \mathbf{i_n} + y_n \mathbf{j_n} + z_0 \mathbf{k_n} - l_2 \mathbf{i_{s1}} - \frac{T_{w2}}{2} \mathbf{j_{s1}} - z_0 \mathbf{k_{s1}} \\
=\ & (x_n - l_2 cos\epsilon_1 + (\tfrac{T_{w2}}{2} cos\phi - z_0 sin\phi) sin\epsilon_1) \mathbf{i_n} \\
& + (y_n - l_2 sin\epsilon_1 - (\tfrac{T_{w1}}{2} cos\phi - z_0 sin\phi) cos\epsilon_1) \mathbf{j_n} \\
& + (z_0 - \tfrac{T_{w2}}{2} sin\phi - z_0 cos\phi) \mathbf{k_n} \\
\equiv\ & r_{x_{t4}} \mathbf{i_n} + r_{y_{t4}} \mathbf{j_n} + r_{z_{t4}} \mathbf{k_n},
\end{aligned}
\tag{75}
$$

20

$$
\begin{aligned}
\mathbf{r_{t5}} &= \mathbf{r_{CG1}} - d_1\mathbf{i_{s1}} - l_3\mathbf{i_{s2}} + \tfrac{T_{w3}}{2}\mathbf{j_{s2}} - z_0\mathbf{k_{s2}} \\
&= x_n\mathbf{i_n} + y_n\mathbf{j_n} + z_0\mathbf{k_n} - d_1\mathbf{i_{s1}} - l_3\mathbf{i_{s2}} + \tfrac{T_{w3}}{2}\mathbf{j_{s2}} - z_0\mathbf{k_{s2}} \\
&= (x_n - (d_1 + l_3cos\epsilon_f + \tfrac{T_{w3}}{2}sin\epsilon_f)cos\epsilon_1 \\
&\quad -((-l_3sin\epsilon_f + \tfrac{T_{w3}}{2}cos\epsilon_f)cos\phi + z_0sin\phi)sin\epsilon_1)\mathbf{i_n} \\
&\quad +(y_n - (d_1 + l_3cos\epsilon_f + \tfrac{T_{w3}}{2}sin\epsilon_f)sin\epsilon_1 \\
&\quad +((-l_3sin\epsilon_f + \tfrac{T_{w3}}{2}cos\epsilon_f)cos\phi + z_0sin\phi)cos\epsilon_1)\mathbf{j_n} \\
&\quad +(z_0 + (-l_3sin\epsilon_f + \tfrac{T_{w3}}{2}cos\epsilon_f)sin\phi - z_0cos\phi)\mathbf{k_n} \\
&\equiv r_{x_{t5}}\mathbf{i_n} + r_{y_{t5}}\mathbf{j_n} + r_{z_{t5}}\mathbf{k_n},
\end{aligned} \tag{76}
$$

and

$$
\begin{aligned}
\mathbf{r_{t6}} &= \mathbf{r_{CG1}} - d_1\mathbf{i_{s1}} - l_3\mathbf{i_{s2}} - \tfrac{T_{w3}}{2}\mathbf{j_{s2}} - z_0\mathbf{k_{s2}} \\
&= x_n\mathbf{i_n} + y_n\mathbf{j_n} + z_0\mathbf{k_n} - d_1\mathbf{i_{s1}} - l_3\mathbf{i_{s2}} - \tfrac{T_{w3}}{2}\mathbf{j_{s2}} - z_0\mathbf{k_{s2}} \\
&= (x_n - (d_1 + l_3cos\epsilon_f - \tfrac{T_{w3}}{2}sin\epsilon_f)cos\epsilon_1 \\
&\quad -((-l_3sin\epsilon_f - \tfrac{T_{w3}}{2}cos\epsilon_f)cos\phi + z_0sin\phi)sin\epsilon_1)\mathbf{i_n} \\
&\quad +(y_n - (d_1 + l_3cos\epsilon_f - \tfrac{T_{w3}}{2}sin\epsilon_f)sin\epsilon_1 \\
&\quad +((-l_3sin\epsilon_f - \tfrac{T_{w3}}{2}cos\epsilon_f)cos\phi + z_0sin\phi)cos\epsilon_1)\mathbf{j_n} \\
&\quad +(z_0 + (-l_3sin\epsilon_f - \tfrac{T_{w3}}{2}cos\epsilon_f)sin\phi - z_0cos\phi)\mathbf{k_n} \\
&\equiv r_{x_{t6}}\mathbf{i_n} + r_{y_{t6}}\mathbf{j_n} + r_{z_{t6}}\mathbf{k_n},
\end{aligned} \tag{77}
$$

respectively. So far we have obtained the position vectors for the external forces. Thus the generalized force Fg_{x_n} is

$$
Fg_{x_n} = \sum_{i=1}^{6} F_{x_{ni}} \cdot \frac{\partial r_{x_{ti}}}{\partial x_n} + \sum_{i=1}^{6} F_{y_{ni}} \cdot \frac{\partial r_{y_{ti}}}{\partial x_n} + \sum_{i=1}^{6} F_{Pi} \cdot \frac{\partial r_{z_{ti}}}{\partial x_n} \tag{78}
$$

Substituting (72), (73), (74), (75), (76) and (77) into (78), we obtain

$$
Fg_{x_n} = F_{x_{n1}} + F_{x_{n2}} + F_{x_{n3}} + F_{x_{n4}} + F_{x_{n5}} + F_{x_{n6}}. \tag{79}
$$

The generalized force associated with the coordinate y_n is

$$
Fg_{y_n} = \sum_{i=1}^{6} F_{x_{ni}} \cdot \frac{\partial r_{x_{ti}}}{\partial y_n} + \sum_{i=1}^{6} F_{y_{ni}} \cdot \frac{\partial r_{y_{ti}}}{\partial y_n} + \sum_{i=1}^{6} F_{Pi} \cdot \frac{\partial r_{z_{ti}}}{\partial y_n} \tag{80}
$$

Substituting (72), (73), (74), (75), (76), and (77) into (80), we obtain

$$
Fg_{y_n} = F_{y_{n1}} + F_{y_{n2}} + F_{y_{n3}} + F_{y_{n4}} + F_{y_{n5}} + F_{y_{n6}}. \tag{81}
$$

The generalized force corresponding to the coordinate ϕ is

$$
Fg_{\phi} = \sum_{i=1}^{6} F_{x_{ni}} \frac{\partial r_{x_{ti}}}{\partial \phi} + \sum_{i=1}^{6} F_{y_{ni}} \frac{\partial r_{y_{ti}}}{\partial \phi} + \sum_{i=1}^{6} F_{Pi} \frac{\partial r_{z_{ti}}}{\partial \phi}, \tag{82}
$$

or we have

$$
\begin{aligned}
Fg_\phi = \ & F_{b1} \cdot (z_0 cos\phi - \tfrac{T_{w1}}{2} sin\phi) + F_{b2} \cdot (z_0 cos\phi + \tfrac{T_{w1}}{2} sin\phi) \\
& + F_{b3} \cdot (z_0 cos\phi - \tfrac{T_{w2}}{2} sin\phi) + F_{b4} \cdot (z_0 cos\phi + \tfrac{T_{w2}}{2} sin\phi) \\
& + (F_{b5} cos\epsilon_f + F_{a5} sin\epsilon_f) \cdot (z_0 cos\phi + (-\tfrac{T_{w3}}{2} cos\epsilon_f + l_3 sin\epsilon_f) sin\phi) \\
& + (F_{b6} cos\epsilon_f + F_{a5} sin\epsilon_f) \cdot (z_0 cos\phi + (\tfrac{T_{w3}}{2} cos\epsilon_f + l_3 sin\epsilon_f) sin\phi) \\
& + F_{P1} \cdot (\tfrac{T_{w1}}{2} cos\phi + z_0 sin\phi) - F_{P2} \cdot (\tfrac{T_{w1}}{2} cos\phi - z_0 sin\phi) \\
& + F_{P3} \cdot (\tfrac{T_{w2}}{2} cos\phi + z_0 sin\phi) - F_{P4} \cdot (\tfrac{T_{w2}}{2} cos\phi - z_0 sin\phi) \\
& + F_{P5} \cdot ((\tfrac{T_{w3}}{2} cos\epsilon_f - l_3 sin\epsilon_f) cos\phi + z_0 sin\phi) \\
& - F_{P6} \cdot ((\tfrac{T_{w3}}{2} cos\epsilon_f + l_3 sin\epsilon_f) cos\phi - z_0 sin\phi).
\end{aligned}
\tag{83}
$$

Similarly, the generalized force for the coordinate ϵ_1 is

$$
Fg_{\epsilon_1} = \sum_{i=1}^{6} F_{xni} \cdot \frac{\partial r_{x_{ti}}}{\partial \epsilon_1} + \sum_{i=1}^{6} F_{yni} \cdot \frac{\partial r_{y_{ti}}}{\partial \epsilon_1} + \sum_{i=1}^{6} F_{Pi} \cdot \frac{\partial r_{z_{ti}}}{\partial \epsilon_1},
\tag{84}
$$

and can be calculated as

$$
\begin{aligned}
Fg_{\epsilon_1} = \ & (F_{b1} + F_{b2}) l_1 - (F_{b3} + F_{b4}) l_2 \\
& - (F_{b5} cos\epsilon_f + F_{a5} sin\epsilon_f) \cdot (\tfrac{S_{w3}}{2} sin\epsilon_f + l_3 cos\epsilon_f + d_1) \\
& - (F_{b6} cos\epsilon_f + F_{a6} sin\epsilon_f) \cdot (-\tfrac{S_{w3}}{2} sin\epsilon_f + l_3 cos\epsilon_f + d_1) \\
& - F_{a1} \cdot (\tfrac{T_{w1}}{2} cos\phi + z_0 sin\phi) + F_{a2} \cdot (\tfrac{T_{w1}}{2} cos\phi - z_0 sin\phi) \\
& - F_{a3} \cdot (\tfrac{T_{w2}}{2} cos\phi + z_0 sin\phi) + F_{a4} \cdot (\tfrac{T_{w2}}{2} cos\phi - z_0 sin\phi) \\
& + (F_{a5} cos\epsilon_f - F_{b5} sin\epsilon_f) \cdot ((-\tfrac{T_{w3}}{2} cos\epsilon_f + l_3 sin\epsilon_f) cos\phi - z_0 sin\phi) \\
& + (F_{a6} cos\epsilon_f - F_{b6} sin\epsilon_f) \cdot ((\tfrac{T_{w3}}{2} cos\epsilon_f + l_3 sin\epsilon_f) cos\phi - z_0 sin\phi).
\end{aligned}
\tag{85}
$$

The generalized force for the coordinate ϵ_f is

$$
Fg_{\epsilon_f} = \sum_{i=1}^{6} F_{xni} \cdot \frac{\partial r_{x_{ti}}}{\partial \epsilon_f} + \sum_{i=1}^{6} F_{yni} \cdot \frac{\partial r_{y_{ti}}}{\partial \epsilon_f} + \sum_{i=1}^{6} F_{Pi} \cdot \frac{\partial r_{z_{ti}}}{\partial \epsilon_f},
\tag{86}
$$

which can be calculated as

$$
\begin{aligned}
Fg_{\epsilon_f} = \ & (F_{a5} cos\epsilon_f - F_{b5} sin\epsilon_f) \cdot (l_3 sin\epsilon_f - \tfrac{T_{w3}}{2} cos\epsilon_f) \\
& + (F_{a6} cos\epsilon_f - F_{b6} sin\epsilon_f) \cdot (l_3 sin\epsilon_f + \tfrac{T_{w3}}{2} cos\epsilon_f) \\
& - (F_{b5} cos\epsilon_f + F_{a5} sin\epsilon_f) \cdot (l_3 cos\epsilon_f + \tfrac{S_{w3}}{2} sin\epsilon_f) \\
& - (F_{b6} cos\epsilon_f + F_{a6} sin\epsilon_f) \cdot (l_3 cos\epsilon_f - \tfrac{S_{w3}}{2} sin\epsilon_f).
\end{aligned}
\tag{87}
$$

Expressions for the generalized forces in (79), (81), (83), *(85)* and (87) are the second important component for the complex model.

6 Subsystems : Tire Model and Suspension Model

6.1 Tire Model

As discussed in the previous section, the longitudinal and lateral components of the tire forces, F_{ai} and F_{bi}, and the suspension forces, F_{pi}, are predicted by the tire model and the suspension model, respectively. In this section we will briefly discuss modeling of tire forces and suspension forces. Modeling the tire/road interaction force is itself an active area of research. For vehicle dynamic simulations purpose, given the road condition and the operating conditions of the tire such as the longitudinal slip ratio, the lateral slip angle and the vertical load of the tire, the tire model will predict both traction/braking force and cornering force generated by the tire (Fig.6).

Road Conditons

Longitudinal Slip Ratio

Lateral Slip Angle

Normal Force

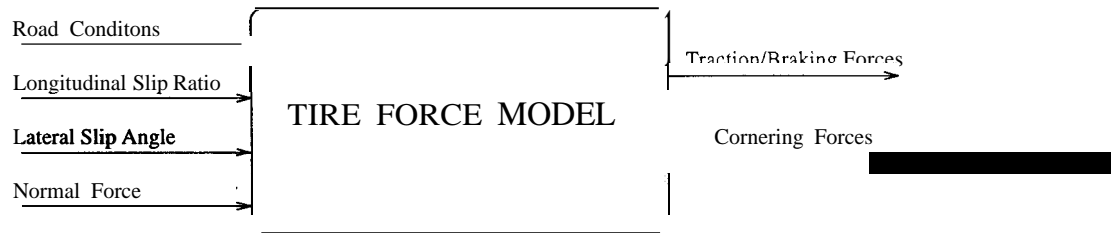TIRE FORCE MODEL

Traction/Braking Forces

Cornering Forces

Figure 6: Tire Force Model

There are two common approaches to the tire force modeling. The first is curve-fitting of the experimental data. This approach can predict a more accurate force traction field. However. the data depends on tire types and it is less portable. One of the most noticeable tire models using data curve fitting techniques is proposed by Pacejka and Bakker (1991). In (Pacejka and Bakker 1991), a set of mathematical equations, known as "magic formulae", are proposed to predict the forces and moments at longitudinal, lateral and camber slip conditions. These formulae and a set of tuning parameters constitute the basis of this model. The second approach is the analytical tire model. One way to analyze the traction field is to divide the tire contact patch into two zones: the sliding zone and the adhesion zone. Shear stresses in the sliding zone of the contact patch are determined by the frictional properties of the tire/road interface. Shear stresses in the adhesion zone are determined by the elastic properties of the tire. For example, the cornering stiffness C_α and longitudinal stiffness C_s represent the first order approximation of the tire force elastic properties. We adopt the second approach at this stage of research and use the tire model by Baraket and Fancher (1989) in the simulation model. This tire model accounts for the influences of tread depth, mean texture depth and skid number on the sliding friction of truck tires The structure of this tire model is summarized in figure 7.

To use this tire force model, tire longitudinal slip ratios and lateral slip angles in terms of vehicle states

are calculated for typical tractor-semitrailer vehicles. The longitudinal slip ratio, X_i is equal to

$$X_i = \begin{cases} \frac{\omega_i r - V}{V} & \text{for braking} \\ \frac{\omega_i r - V_i}{\omega_i r_i} & \text{for traction} \end{cases}$$

where V is the forward velocity, w_i is the angular velocity and r is the radius of the $i-th$ wheel. The lateral slip angle, α_i, is equal to

$$
\begin{aligned}
\alpha_1 &= \delta - tan^{-1}\left(\frac{\dot{y}_u + l_1 \dot{\epsilon}_1}{\dot{x}_u - \frac{T_{w1}}{2}\dot{\epsilon}_1}\right) \\
\alpha_2 &= \delta - tan^{-1}\left(\frac{\dot{y}_u + l_1 \dot{\epsilon}_1}{\dot{x}_u + \frac{T_{w1}}{2}\dot{\epsilon}_1}\right) \\
\alpha_3 &= -tan^{-1}\left(\frac{\dot{y}_u - l_2 \dot{\epsilon}_1}{\dot{x}_u - \frac{T_{w2}}{2}\dot{\epsilon}_1}\right) \\
\alpha_4 &= -tan^{-1}\left(\frac{\dot{y}_u - l_2 \dot{\epsilon}_1}{\dot{x}_u + \frac{T_{w2}}{2}\dot{\epsilon}_1}\right) \\
\alpha_5 &= -tan^{-1}\left(\frac{-\dot{x}_u sin\epsilon_f + (\dot{y}_u - d_1 \dot{\epsilon}_1)cos\epsilon_f - l_3(\dot{\epsilon}_1 + \dot{\epsilon}_f)}{\dot{x}_u cos\epsilon_f + (\dot{y}_u - d_1 \dot{\epsilon}_1)sin\epsilon_f - \frac{T_{w3}}{2}(\dot{\epsilon}_1 + \dot{\epsilon}_f)}\right) \\
\alpha_6 &= -tan^{-1}\left(\frac{-\dot{x}_u sin\epsilon_f + (\dot{y}_u - d_1 \dot{\epsilon}_1)cos\epsilon_f - l_3(\dot{\epsilon} + \dot{\epsilon}_f)}{\dot{x}_u cos\epsilon_f + (\dot{y}_u - d_1 \dot{\epsilon}_1)sin\epsilon_f + \frac{T_{w3}}{2}(\dot{\epsilon}_1 + \dot{\epsilon}_f)}\right)
\end{aligned}
\tag{88}
$$

PAVEMENT PARAMETERS

SN40- Skid number

MD - Mean texture depth

TIRE CONDITION

Gd - Tread groove depth

PAVEMENT INFLUENCE

μ_{xp} -Peak data value

μ_{xs} - Sliding data value

TIRE DATA
Flatbed

FRICTION MODEL

μ

αSx

SIMULATION VALUES

Fz - Vertical load

V - Vehicle speed

PROCESSING TIRE DATA

Cs - Longitudinal stiffness

Ca - Cornering stiffness

a/l - Pressure distribution

TIRE MODEL

Fy

α

α - Slip angle

Sx - Longitudinal Slip

PREDICTION OF TRACTION

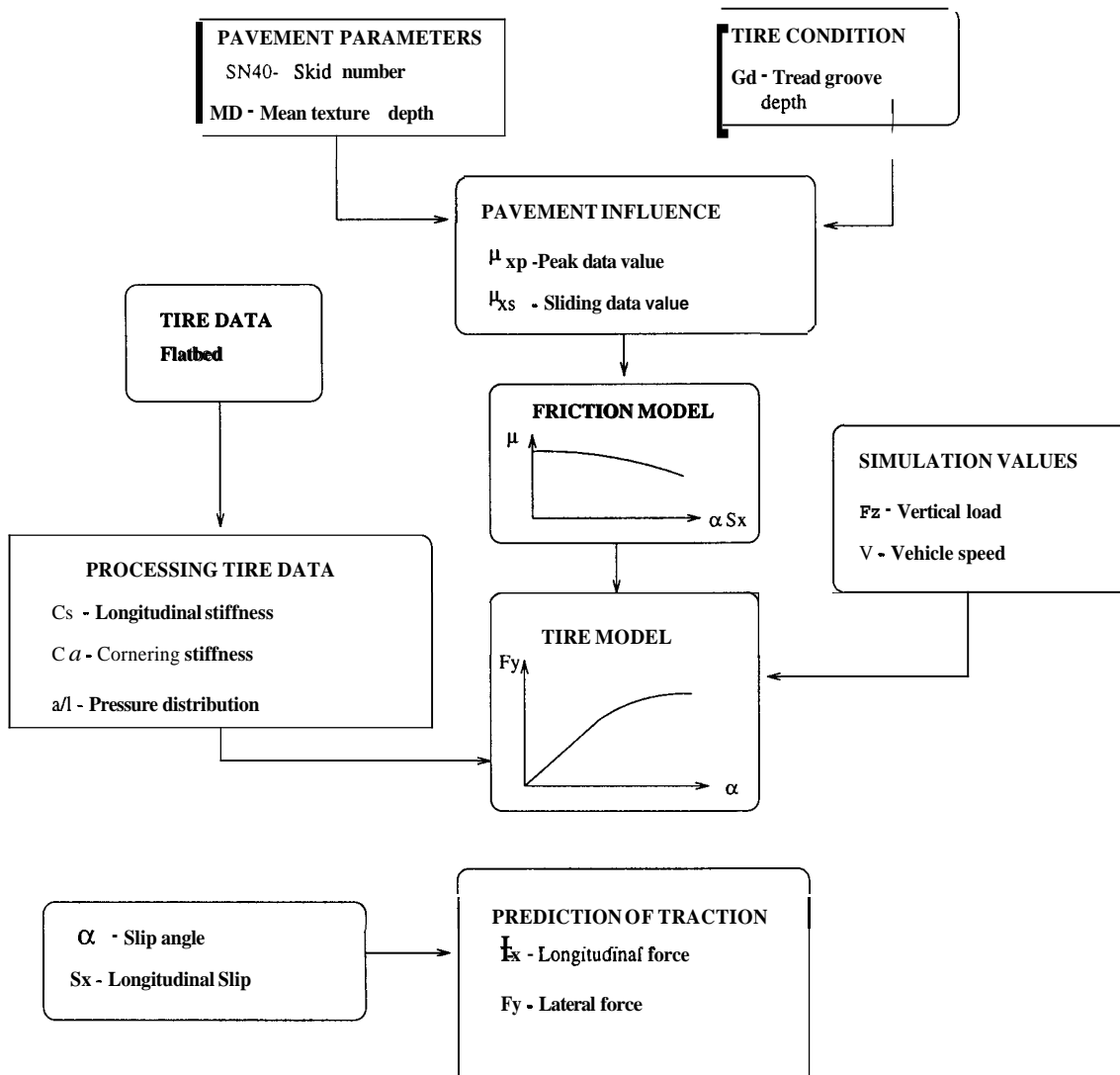Fx - Longitudinal force

Fy - Lateral force

Figure 7: **Comprehensive Tire Model (Baraket and Fancher)**

25

6.2 Suspension Model

By far the majority of commercial vehicle suspensions employ the leaf spring as the vertically compliant element. For the sake of simplicity, instead of using experimental suspension data, we will adopt an analytical approach to model the suspension **as** the combination of a nonlinear spring and a damper element. **As** shown in Fig. 8, the vertical force acting on the vehicle sprung mass through the suspension system is equal to the static equilibrium force plus the perturbation force, which is denoted as F_s, from the spring equilibrium point. The perturbation force can be modeled as

$$F_{si} = \begin{cases} K_{f1}e_i + K_{f2}e_i^5 + D_f\dot{e}_i & \text{for } i = 1,2 \\ K_{r1}e_i + K_{r2}e_i^5 + D_r\dot{e}_i & \text{for } i = 3,4 \\ K_{t1}e_i + K_{t2}e_i^5 + D_t\dot{e}_i & \text{for } i = 5,6 \end{cases} \tag{89}$$

where K_{f1} and K_{f2} are parameters of the tractor front spring, K_{r1} and K_{r2} are parameters of the tractor rear spring, K_{t1} and K_{t2} are parameters of the trailer spring, D_f, D, and D_t are parameters for dampers, and e_i is the deflection of the $i - th$ spring from its equilibrium position and is given as

$$e_1 = -\frac{T_{w1}}{2}\phi$$
$$e_2 = \frac{T_{w1}}{2}\phi$$
$$e_3 = -\frac{T_{w2}}{2}\phi$$
$$e_4 = \frac{T_{w1}}{2}\phi$$
$$e_5 = -(\frac{T_{w3}}{2}\phi)cos\epsilon_f + (l_3\phi)sin\epsilon_f$$
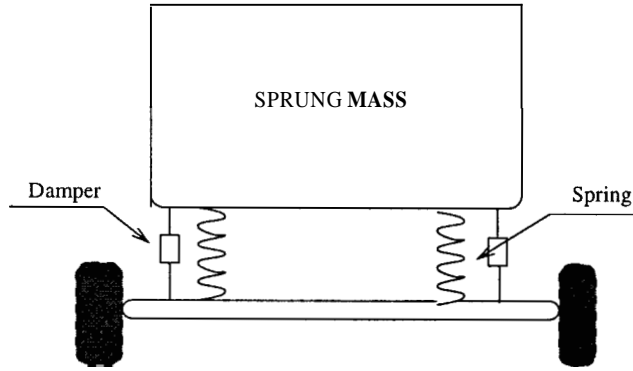$$e_6 = (\frac{T_{w3}}{2}\phi)cos\epsilon_f + (l_3\phi)sin\epsilon_f$$

Figure 8: Suspension Model

7 Model Verification: Simulation and Experimental Results

In this section, simulation results of the complex vehicle model will be compared with the open loop experimental results obtained from field tests. The test vehicle is a class 8 tractor-semitrailer truck. The test truck was operated under fixed speed cruise control and a step steering command was given manually by the driver. The radius of curvature of the test track is approximately 80 meters. Measured signals for the handling tests include lateral acceleration, yaw rate, roll angle of the sprung mass, articulation angle between the tractor and the semitrailer, and the front wheel steering angle. In order to compare the simulation results of the complex vehicle model with the test vehicle, the front wheel steering angle which is recorded during experiments is used as the steering input for the simulation model. Furthermore, simulations are performed using the test vehicle parameters listed in Tables 2, **3** and **4.** Some of the parameters are measured values and some are estimated values. Simulation results of the complex model and the experimental results of the test vehicle are compared in Figs. 9, 10, **11** and 12, respectively. In general, the predicted simulation results agree well with the field test data. We observe that the predicted response of the articulation angle between the tractor and the trailer is slower than the actual response. The discrepencies between the predicted responses and the test results may be attributed to:

1. some unkown vehicle parameters, e.g. the moment of inertia, tire cornering stiffness, the height of the roll center and the height of the vertical C.G.,

2. effects of dual tires and tandem axes, which impose nonholonomic constraints on the vehicle motion,

3. unmodeled dynamics, including roll steer and chassis compliance effect,

4. sensor calibration errors in instrumentation.

27

parameter	unit	value	parameter	unit	value
m_1	Kg	8444.0	m_2	Kg	23472.0
I_{x1}	$Kg - m^2$	12446.5*	I_{x2}	$Kg - m^2$	35523.7*
I_{y1}	$Kg - m^2$	65734.6*	I_{y2}	$Kg - m^2$	181565.5*
I_{z1}	$Kg - m^2$	65734.6*	I_{y2}	$Kg - m^2$	181565.5*
l_1	m	2.59	T_{w1}	m	2.02
l_2	m	3.29	T_{w2}	m	1.82
l_3	m	9.65	T_{w3}	m	1.82
z_0	m	1.20*	h_2	m	0.20*
d_1	m	3.06	d_3	m	4.20
d_2	m	0.60*	d_4	m	1.20*

Table 2: Parameters for a Tractor-Semitrailer Vehicle
(Parameters marked with an asterisk are estimated values)

parameter	unit	value	parameter	unit	value
K_{f1}	N/m	2.72e5*	K_{f2}	N/m^5	3.36e10*
K_{r1}	N/m	8.53e5*	K_{r2}	N/m^5	1.05e11*
K_{t1}	N/m	1.55e6*	K_{t2}	N/m^5	1.92e12*
D_f	$N \cdot sec/m$	9080*	D_r	$N \cdot sec/m$	9080*
D_t	$N \cdot sec/m$	9080*			

Table 3: Suspension Parameters

parameter	unit	value	parameter	unit	value
I_w	$Kg - m^2$	13.15*	R	m	0.3*
C_{α_f}	N/rad	143330.0	C_{lf}	N	127120.0
C_{α_r}	N/rad	143330.0 x 4	C_{lr}	N	108960.0 x 4
C_{α_t}	N/rad	80312.0 x 4	C_{lt}	N	95340.0 x 4

Table 4: Tire and Wheel Parameters

28

solid line: experiment, dashdot line: simulation
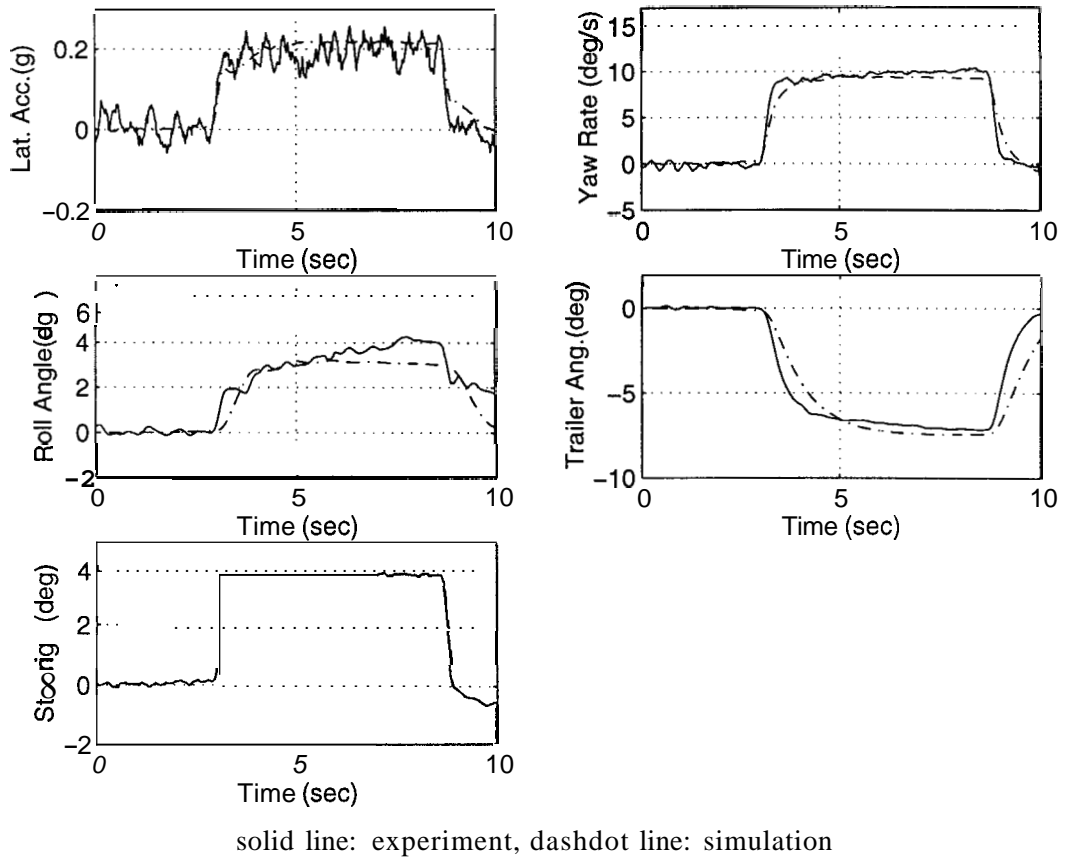
Figure 9: Step input response with the longitudinal vehicle speed **30 MPH**,

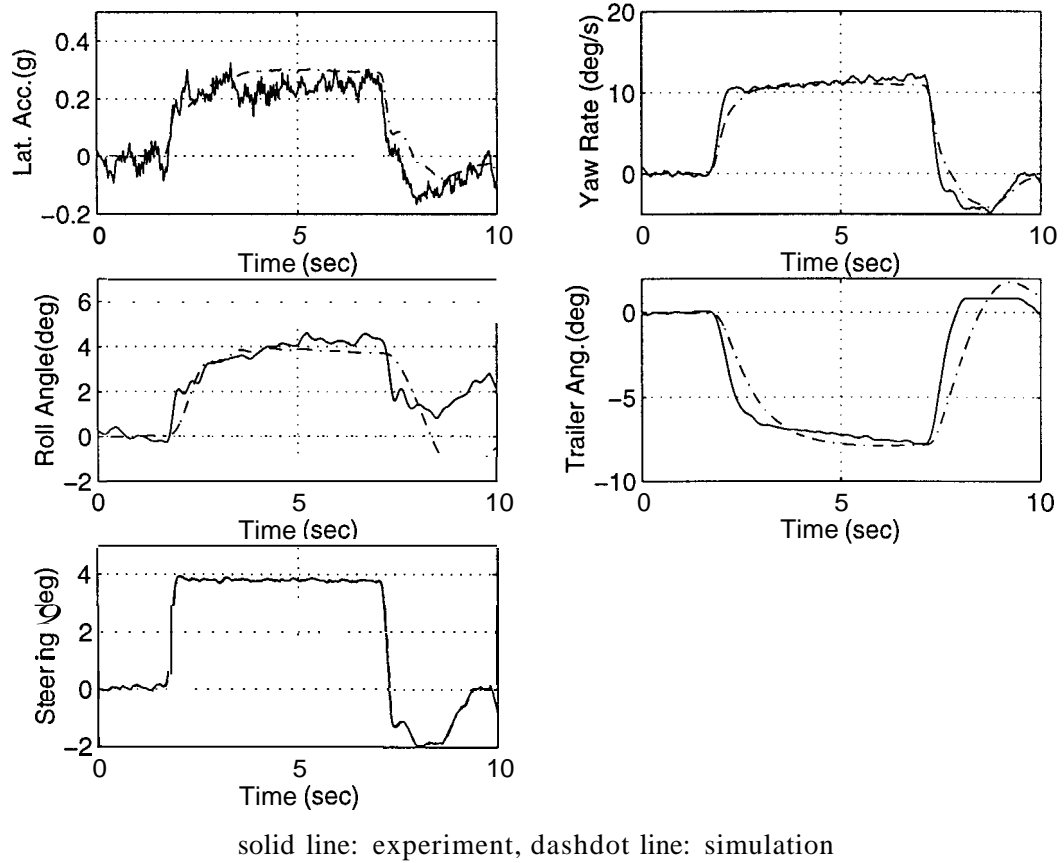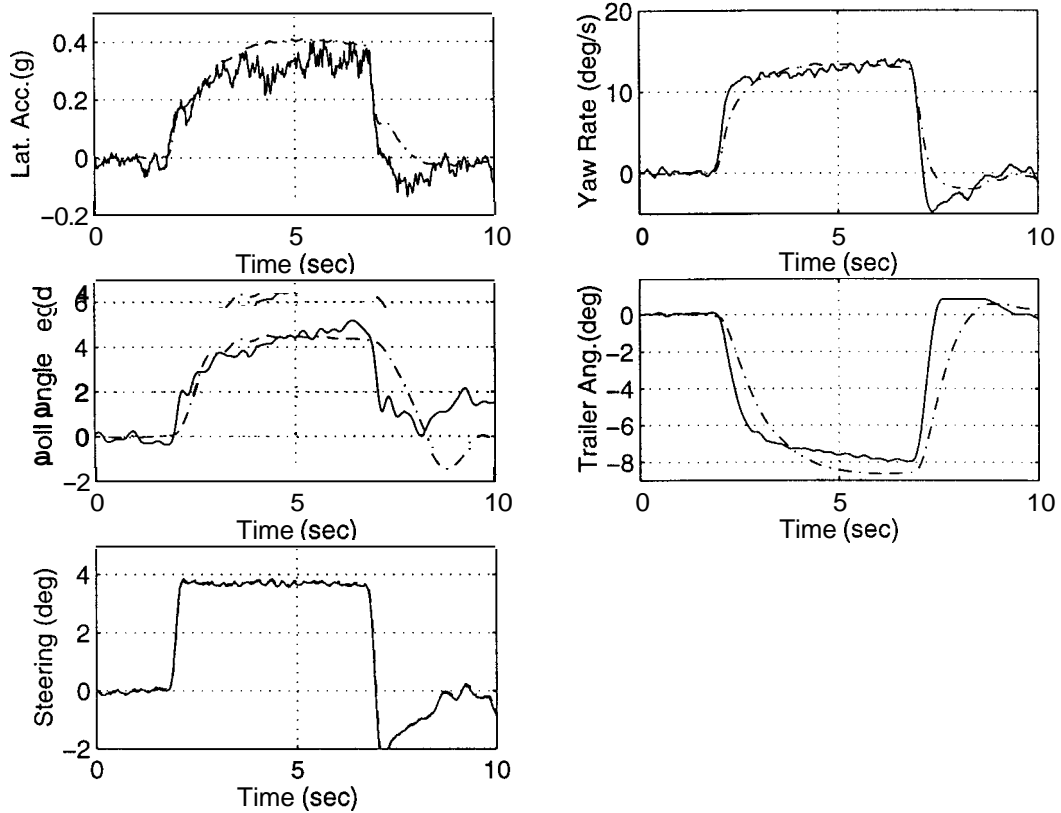solid line: experiment, dashdot line: simulation

Figure 10: Step input response with the longitudinal vehicle speed **35** MPH

solid line: experiment, dashdot line: simulation

Figure 11: Step input response with the longitudinal vehicle speed 40 MPH
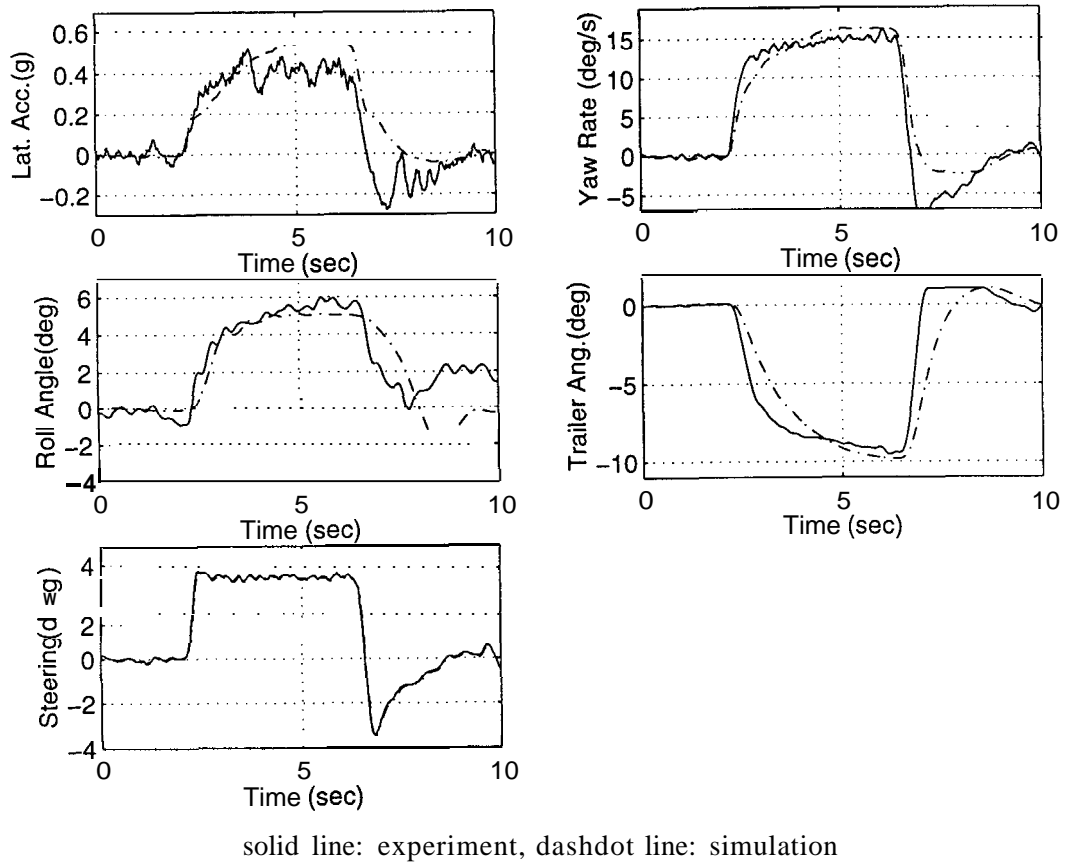
solid line: experiment, dashdot line: simulation

Figure 12: Step input response with the longitudinal vehicle speed 46 MPH
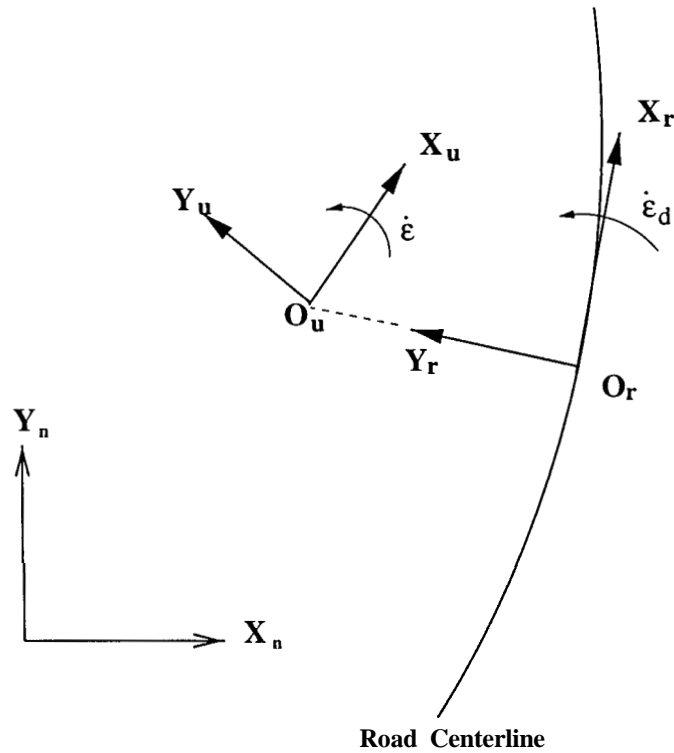
8 Road reference frame

Figure 13: Unsprung Mass and Road Reference Coordinates

In previous sections, the vehicle model was derived with respect to the unsprung mass reference frame. Since one of the objectives for lateral control of automated vehicles is to follow the road, the description of the relative position and the relative orientation of the controlled vehicle with respect to the road centerline need to be given explicitly. To this end, the road reference coordinate $OrXrYr$ in Fig.13 is naturally introduced to describe tracking errors of the vehicle with respect to the road centerline. The road reference frame is defined such that the X_r axis is tangent to the road centerline and the Y_r axis passes through the vehicle C.G. Once the road reference frame is defined, the vehicle model with respect to the road reference frame can be obtained by state variable transformation from the vehicle model with respect to the unsprung mass reference frame. By equating two expressions for the vehicle velocity, one in the unsprung mass reference frame and the other in the road reference frame, we obtain the velocity transformation equations between the unsprung mass reference frame and th eroad reference frame. Similarly, by equating two expressions for the vehicle acceleration, one in the unsprung mass reference frame and the other in the road reference frame, we obtain the acceleration transformation equations between the unsprung mass reference frame and the road reference frame.

Recall from section 2 that the vehicle velocity at C.G. can be expressed as

$$\mathbf{V_{CG}} = \dot{x}_u \mathbf{i_u} + \dot{y}_u \mathbf{j_u}, \tag{90}$$

where $\dot{x}_u$ and $\dot{y}_u$ are velocity components of the vehicle along the X_u axis and Y_u axis of the unsprung mass coordinate, respectively. The vehicle acceleration can be expressed as

$$\mathbf{a_{CG}} = (\ddot{x}_u - \dot{y}_u \dot{\epsilon}_1)\mathbf{i_u} + (\ddot{y}_u + \dot{x}_u \dot{\epsilon}_1)\mathbf{j_u}, \tag{91}$$

where $\dot{\epsilon}_1$ is the yaw rate of the unsprung mass reference frame.

On the other hand, the vehicle velocity $\mathbf{V_{CG}}$ and the vehicle acceleration $\mathbf{a_{CG}}$ at C.G. can also be obtained in coordinates of the road reference frame $X_r Y_r Z_r$. From Fig. 13 and by the definition of the road reference frame $X_r Y_r Z_r$ such that the Y_r axis always passes through the vehicle C.G., the position of the vehicle C.G. with respect to the road reference frame $X_r Y_r Z_r$ is

$$\mathbf{r_{CG/Or}} = y_r \mathbf{j_r}, \tag{92}$$

then the vehicle velocity with respect to $X_r Y_r Z_r$ is

$$\mathbf{V_{CG/Or}} = \dot{y}_r \mathbf{j_r} + y_r \frac{d}{dt}\mathbf{j_r}. \tag{93}$$

Since the angular velocity of the $X_r Y_r Z_r$ frame is $\dot{\epsilon}_d \mathbf{k_r}$, we have

$$\frac{d}{dt}\mathbf{i_r} = \dot{\epsilon}_d \mathbf{j_r} \tag{94}$$

and

$$\frac{d}{dt}\mathbf{j_r} = -\dot{\epsilon}_d \mathbf{i_r}. \tag{95}$$

Substituting (95) into (93), we obtain the vehicle velocity with respect to the road reference frame as

$$\mathbf{V_{CG/Or}} = \dot{y}_r \mathbf{j_r} - y_r \dot{\epsilon}_d \mathbf{i_r} \tag{96}$$

Since the road reference frame $X_r Y_r Z_r$ is moving with velocity

$$\mathbf{V_{Or}} = \dot{x}_r \mathbf{i_r}, \tag{97}$$

the vehicle absolute velocity is

$$\mathbf{V_{CG}} = \mathbf{V_{CG/Or}} + \mathbf{V_{Or}} = (\dot{x}_r - y_r \dot{\epsilon}_d)\mathbf{i_r} + \dot{y}_r \mathbf{j_r}, \tag{98}$$

where $\mathbf{V_{CG/Or}}$ and $\mathbf{V_{Or}}$ are given in (96) and (97), respectively. The acceleration in the road reference frame coordinates can be obtained by differentiating (98),

$$\begin{aligned}
\mathbf{a_{CG}} &= (\ddot{x}_r - \dot{y}_r \dot{\epsilon}_d - y_r \ddot{\epsilon}_d)\mathbf{i_r} + \ddot{y}_r \mathbf{j_r} + (\dot{x}_r - y_r \dot{\epsilon}_d)\frac{d}{dt}\mathbf{i_r} + \dot{y}_y \frac{d}{dt}\mathbf{j_r} \\
&= (\ddot{x}_r - 2\dot{y}_r \dot{\epsilon}_d - y_r \ddot{\epsilon}_d)\mathbf{i_r} + (\ddot{y}_r + \dot{x}_r \dot{\epsilon}_d - y_r \dot{\epsilon}_d^2)\mathbf{j_r}
\end{aligned} \tag{99}$$

34

where (94) and (95) are used in (99). Furthermore, the transformation matrix from the road reference frame to the unsprung mass reference is

$$\begin{pmatrix} \mathbf{i_r} \\ \mathbf{j_r} \end{pmatrix} = \begin{pmatrix} \cos \epsilon_r & -\sin \epsilon_r \\ \sin \epsilon_r & \cos \epsilon_r \end{pmatrix} \begin{pmatrix} \mathbf{i_u} \\ \mathbf{j_u} \end{pmatrix} \tag{100}$$

If the relative yaw angle ϵ_r is small, (100) can be approximated as

$$\begin{aligned} \mathbf{i_r} &= \cos\epsilon_r \mathbf{i_u} - \sin\epsilon_r \mathbf{j_u} \\ &\simeq \mathbf{i_u} - \epsilon_r \mathbf{j_u} \end{aligned} \tag{101}$$

and

$$\begin{aligned} \mathbf{j_r} &= \sin\epsilon_r \mathbf{i_u} + \cos\epsilon_r \mathbf{j_u} \\ &\simeq \epsilon_r \mathbf{i_u} + \mathbf{j_u}. \end{aligned} \tag{102}$$

Substituting (101) and (102) into (98), we obtain

$$\begin{aligned} \mathbf{V_{CG}} &= (\dot{x}_r - y_r \dot{\epsilon}_d)\mathbf{i_r} + \dot{y}_r \mathbf{j_r} \\ &\simeq (\dot{x}_r - y_r \dot{\epsilon}_d + \dot{y}_r \epsilon_r)\mathbf{i_u} + (\dot{y}_r - \dot{x}_r \epsilon_r + y_r \epsilon_r \dot{\epsilon}_d)\mathbf{j_u} \end{aligned} \tag{103}$$

Similarly, by substituting (101) and (102) into (99), we obtain

$$\begin{aligned} \mathbf{a_{CG}} &= (\ddot{x}_r - y_r \ddot{\epsilon}_d - 2\dot{y}_r \dot{\epsilon}_d)\mathbf{i_r} + (\ddot{y}_r - y_r \dot{\epsilon}_d^2 + \dot{x}_r \dot{\epsilon}_d)\mathbf{j_r} \\ &\simeq (\ddot{x}_r - y_r \ddot{\epsilon}_d - 2\dot{y}_r \dot{\epsilon}_d + \ddot{y}_r \epsilon_r - y_r \epsilon_r \dot{\epsilon}_d^2 + \dot{x}_r \epsilon_r \dot{\epsilon}_d)\mathbf{i_u} \\ &\quad + (\ddot{y}_r - y_r \dot{\epsilon}_d^2 + \dot{x}_r \dot{\epsilon}_d - \ddot{x}_r \epsilon_r + y_r \epsilon_r \ddot{\epsilon}_d + 2\dot{y}_r \dot{\epsilon}_d \epsilon_r)\mathbf{j_u}. \end{aligned} \tag{104}$$

By neglecting third and higher order terms, Eqs. (103) and (104) can be further simplified as

$$\mathbf{V_{CG}} \simeq (\dot{x}_r - y_r \dot{\epsilon}_d + \dot{y}_r \epsilon_r)\mathbf{i_u} + (\dot{y}_r - \dot{x}_r \epsilon_r)\mathbf{j_u} \tag{105}$$

and

$$\mathbf{a_{CG}} \simeq (\ddot{x}_r - y_r \ddot{\epsilon}_d - 2\dot{y}_r \dot{\epsilon}_d + \ddot{y}_r \epsilon_r + \dot{x}_r \epsilon_r \dot{\epsilon}_d)\mathbf{i_u} + (\ddot{y}_r + \dot{x}_r \dot{\epsilon}_d - \ddot{x}_r \epsilon_r)\mathbf{j_u}, \tag{106}$$

respectively. By equating Eqs. (90) and (105), we obtain

$$\dot{x}_u \simeq \dot{x}_r - y_r \dot{\epsilon}_d + \dot{y}_r \epsilon_r \tag{107}$$

and

$$\dot{y}_u \simeq \dot{y}_r - \dot{x}_r \epsilon_r. \tag{108}$$

Similarly, by equating Eqs. (91) and (106), we obtain

$$\ddot{x}_u - \dot{y}_u \dot{\epsilon}_1 \simeq \ddot{x}_r - y_r \ddot{\epsilon}_d - 2\dot{y}_r \dot{\epsilon}_d + \ddot{y}_r \epsilon_r + \dot{x}_r \epsilon_r \dot{\epsilon}_d \tag{109}$$

and

$$\ddot{y}_u - \dot{x}_u \dot{\epsilon}_1 \simeq \ddot{y}_r + \dot{x}_r \dot{\epsilon}_d - \ddot{x}_r \epsilon_r. \tag{110}$$

Substituting (108) into (109) and noting

$$\dot{\epsilon}_1 = \dot{\epsilon}_r + \dot{\epsilon}_d \tag{111}$$

we obtain

$$\ddot{x}_u \simeq \ddot{x}_r - y_r \ddot{\epsilon}_d - \dot{y}_r \dot{\epsilon}_d + \dot{y}_r \dot{\epsilon}_r + \ddot{y}_r \epsilon_r - \dot{x}_r \epsilon_r \dot{\epsilon}_r. \tag{112}$$

Similarly by substituting (107) into (110) we obtain

$$\ddot{y} = \ddot{y} - \dot{x}_r \dot{\epsilon}_r - \ddot{x}_r \epsilon_r. \tag{113}$$

Eqs. (107), (108), (112) and (113) will be used to formulate lateral control models in section 9.

9   Steering Control Model (SIM1)

The steering control model will be constructed in two steps. First, a 3 d.o.f. (6 states) model is simplified from the complex model. Next, the simplified model is transformed with respect to the road reference coordinate, which is discussed in section 8. For the nomenclature of the simplified models, refer to Table 5.

9.1   Model Simplification

The following assumptions are made to simplify the complex model to one with only lateral and yaw dynamics.

- *o* The roll motion is negligible.

- *o* The longitudinal acceleration x_r is small.

- *o* The relative yaw angle ϵ_r of the tractor with respect to the road centerline is small.

- *o* The relative yaw angle ϵ_f of the tractor and the trailer is small.

- ● Tire slip angles of the left and the right wheels are the same.

- *o* Tire longitudinal and lateral forces are represented by the linearized tire model.

parameter	description
Y_r	lateral displacement of the tractor C.G. from the road center line
ϵ_r	relative yaw angle of the tractor w.r.t. road center line
ϵ_f	relative yaw angle of the tractor and the trailer
ρ	radius of curvature of the road
$\dot{\epsilon}_d$	desired yaw rate set by the road and is equal to $\frac{\dot{x}}{\rho}$
δ	tractor front wheel steering angle
F_1	braking force on the trailer left wheel
F_2	braking force on the trailer left wheel
λ_i	longitudinal slip ratio
α_i	lateral slip angle
m_1	tractor mass
I_{z1}	tractor moment of inertia
m_2	semitrailer mass
I_{z2}	semitrailer's moment of inertia
l_1	distance between tractor C.G. and front wheel axle
l_2	distance between tractor C.G. and real wheel axle
l_3	distance between joint (fifth wheel) and trailer real wheel axle
D_1	relative position between tractor's C.G. to fifth wheel
D_3	relative position between semitrailer's C.G. to fifth wheel
T_{w3}	semitrailer rear axle track width
$C_{\alpha f}$	cornering stiffness of tractor front wheel
$C_{\alpha r}$	cornering stiffness of tractor rear wheel
$C_{\alpha t}$	cornering stiffness of semitrailer rear wheel
Sx_f	longitudinal stiffness of tractor front wheel
Sx_r	longitudinal stiffness of tractor rear wheel
Sx_t	longitudinal stiffness of semitrailer rear wheel

Table 5: Nomenclature of Control Models

By using the above assumptions, the complex vehicle model in section **4** can be simplified **as**

$$
\begin{aligned}
&(m_1 + m_2)\ddot{y}_u - m_2(d_1 + d_3 cos\epsilon_f)\ddot{\epsilon}_1 - m_2 d_3 cos\epsilon_f \ddot{\epsilon}_f \\
&+ (m_1 + m_2)\dot{x}_u \dot{\epsilon}_1 + m_2 d_3 sin\epsilon_f (\dot{\epsilon}_1 + \dot{\epsilon}_f)^2 \\
&= F_{b1} + F_{b2} + F_{b3} + F_{b4} + F_{b5} + F_{b6},
\end{aligned}
\tag{114}
$$

$$
\begin{aligned}
&-m_2(d_1 + d_3 cos\epsilon_f)\ddot{y}_u + (I_{z1} + I_{z2} + m_2(d_1 + d_3 cos\epsilon_f)^2)\ddot{\epsilon}_1 \\
&+ (I_{z2} + m_2 d_3^2 + m_2 d_1 d_3 cos\epsilon_f)\ddot{\epsilon}_f \\
&- m_2(d_1 + d_3 cos\epsilon_f)\dot{x}_u \dot{\epsilon}_1 - m_2 d_3 sin\epsilon_f \dot{y}_u \dot{\epsilon}_1 \\
&- 2m_2 d_1 d_3 sin\epsilon_f \dot{\epsilon}_1 \dot{\epsilon}_f - m_2 d_1 d_3 sin\epsilon_f \dot{\epsilon}_f^2 \\
&= (F_{b1} + F_{b2})l_1 - (F_{b3} + F_{b4})l_2 - (F_{b5} + F_{b6})(d_1 + l_3) \\
&+ (F_{a2} - F_{a1})\tfrac{T_{w1}}{2} + (F_{a4} - F_{a3})\tfrac{T_{w2}}{2} + (F_{a6} - F_{a5})\tfrac{T_{w3}}{2},
\end{aligned}
\tag{115}
$$

and

$$
\begin{aligned}
&-m_2 d_3 cos\epsilon_f \ddot{y}_u + (I_{z2} + m_2 d_3^2 + m_2 d_1 d_3 cos\epsilon_f)\ddot{\epsilon}_1 + (I_{z2} + m_2 d_3^2)\ddot{\epsilon}_f \\
&- m_2 d_3 cos\epsilon_f \dot{x}_u \dot{\epsilon}_1 - m_2 d_3 sin\epsilon_f \dot{y}_u \dot{\epsilon}_1 + m_2 d_1 d_3 sin\epsilon_f \dot{\epsilon}_1^2 \\
&= -(F_{b5} + F_{b6})l_3 + (F_{a6} - F_{a5})\tfrac{T_{w3}}{2}.
\end{aligned}
\tag{116}
$$

To obtain the steering control model (SIM1), we notice that longitudinal tire forces, F_{ai}, in (114), (115) and (116) are zero under no braking and lateral tire forces, F_{bi}, can be represented by the linearized tire model,

$$
F_{bi} = \begin{cases} C_{\alpha_f}\alpha_f & for \quad i = 1,2 \\ C_{\alpha_r}\alpha_f & for \quad i = 3,4 \\ C_{\alpha_t}\alpha_f & for \quad i = 5,6 \end{cases},
\tag{117}
$$

where lateral slip angles α_f a_r and α_t are

$$
\alpha_f \simeq \delta - \frac{\dot{y}_u + l_1\dot{\epsilon}_1}{\dot{x}_u},
$$

$$
\alpha_r \simeq -\frac{\dot{y}_u - l_2\dot{\epsilon}_1}{\dot{x}_u},
$$

and

$$
\alpha_t \simeq -\frac{\dot{y}_u - d_1\dot{\epsilon}_1 - l_3(\dot{\epsilon}_1 + \dot{\epsilon}_f)}{\dot{x}_u} + \epsilon_f,
$$

respectively. Substituting F_{bi} in (11) into the simplified vehicle model (114), (11.5) and (116), we obtain the control model (SIM1) **as**

$$
M\ddot{q} + C(q, \dot{q}) + D\dot{q} + Kq = F\delta,
\tag{118}
$$

38

where

$$q = [y_u, \epsilon_1, \epsilon_f]^T$$

is the generalized coordinate vector,

$$M = \begin{pmatrix} m_1 + m_2 & -m_2(d_1 + d_3 cos\epsilon_f) & -m_2 d_3 cos\epsilon_f \\ -m_2(d_1 + d_3 cos\epsilon_f) & I_{z1} + I_{z2} + m_2(d_1^2 + d_3^2) + 2m_2 d_1 d_3 cos\epsilon_f & I_{z2} + m_2 d_3^2 cos\epsilon_f \\ -m_2 d_3 cos\epsilon_f & I_{z2} + m_2 d_3^2 + m_2 d_1 d_3 cos\epsilon_f & I_{z2} + m_2 d_3^2 \end{pmatrix}$$

is the inertial matrix,

$$C(q, \dot{q}) = \begin{pmatrix} (m_1 + m_2)\ddot{x}_u + m_2 d_3 sin\epsilon_f(\dot{\epsilon}_1 + \dot{\epsilon}_f)^2 \\ -m_2(d_1 + d_3 cos\epsilon_f)\dot{x}_u\dot{\epsilon}_1 - m_2 d_3 sin\epsilon_f \dot{y}_u\dot{\epsilon}_1 - 2m_2 d_1 d_3 sin\epsilon_f \dot{\epsilon}_1\dot{\epsilon}_f - m_2 d_1 d_3 sin\epsilon_f \dot{\epsilon}_f^2 \\ -m_2 d_3 sin\epsilon_f \dot{y}_u\dot{\epsilon}_1 - m_2 d_3 cos\epsilon_f \dot{x}_u\dot{\epsilon}_1 + m_2 d_1 d_3 sin\epsilon_f \dot{\epsilon}_1^2 \end{pmatrix}$$

is the vector of the Coriolis and Centrifugal forces,

$$D = \frac{2}{\dot{x}} \begin{pmatrix} C_{af} + C_{ar} + C_{at} & l_1 C_{af} - l_2 C_{ar} - (l_3 + d_1)C_{at} & -l_3 C_{at} \\ l_1 C_{af} - l_2 C_{ar} - (l_3 + d_1)C_{at} & l_1^2 C_{af} + l_2^2 C_{ar} + (l_3 + d_1)^2 C_{at} & l_3(l_3 + d_1)C_{at} \\ -l_3 C_{at} & l_3(l_3 + d_1)C_{at} & l_3^2 C_{at} \end{pmatrix}$$

is the damping matrix,

$$K = \begin{pmatrix} 0 & 0 & -2C_{at} \\ 0 & 0 & 2(l_3 + d_1)C_{at} \\ 0 & 0 & 2l_3 C_{at} \end{pmatrix}$$

is the potential matrix, and the vector $F \in R^{3 \times 1}$ is

$$F = 2\, C_{af} \cdot [1,\ l_1,\ 0]^T$$

Eq. (118) represents the simplified vehicle model with respect to the unsprung mass reference coordinate.

9.2 Control Model with respect to the Road Reference Frame

Recall from section 8 that state variables with respect to the unsprung mass reference frame can be transformed into state variables with respect to the road reference frame by

$$y_u = \dot{y}_r - \dot{x}_r \epsilon_r, \tag{119}$$

$$\ddot{y}_u = \ddot{y}_r - \dot{x}_r \dot{\epsilon}_r - \ddot{x}_r \epsilon_r, \tag{120}$$

$$\dot{\epsilon}_1 = \dot{\epsilon}_r + \dot{\epsilon}_d \tag{121}$$

and

$$\ddot{\epsilon}_1 = \ddot{\epsilon}_r + \ddot{\epsilon}_d. \tag{122}$$

By the assumptions that the longitudinal acceleration $\ddot{x}_r$ and the relative yaw angle ϵ_r are small, their product in (120) can be neglected. Substituting the state variable transformation equations (119), (120), (121) and (122) into the control model (118), we obtain

$$M\ddot{q}_r + \Phi(q_r, \dot{q}_r, \dot{\epsilon}_d, \ddot{\epsilon}_d) = F\delta, \tag{123}$$

where

$$q_r = [y_r, \ \epsilon_r, \ \epsilon_f]^T$$

is the vector of state variables with respect to road centerline and is defined in Table 5, $\Phi(q_r, \dot{q}_r, \dot{\epsilon}_d, \ddot{\epsilon}_d) \in R^{3\times1}$ is the vector with its components

$\Phi(q_r, \dot{q}_r, \dot{\epsilon}_d, \ddot{\epsilon}_d)(1) =$
$$\begin{pmatrix} \frac{2}{\dot{x}}((C_{\alpha f} + C_{\alpha r} + C_{\alpha t})(\dot{y}_r - \dot{x}\epsilon_r) + (l_1 C_{\alpha f} - l_2 C_{\alpha r} - (l_3 + d_1)C_{\alpha t})(\dot{\epsilon}_r + \dot{\epsilon}_d) - l_3 C_{\alpha t}\dot{\epsilon}_f) \\ -2C_{\alpha t}\epsilon_f + m_2 d_3 sin\epsilon_f(\dot{\epsilon}_r + \dot{\epsilon}_d + \dot{\epsilon}_f)^2 + (m_1 + m_2)\dot{x}\dot{\epsilon}_d - m_2(d_1 + d_3 cos\epsilon_f)\ddot{\epsilon}_d \end{pmatrix}$$

$\Phi(q_r, \dot{q}_r, \dot{\epsilon}_d, \ddot{\epsilon}_d)(2) =$
$$\begin{pmatrix} \frac{2}{\dot{x}}((l_1 C_{\alpha f} - l_2 C_{\alpha r} - (l_3 + d_1)C_{\alpha t})(\dot{y}_r - \dot{x}\epsilon_r) + (l_1^2 C_{\alpha f} + l_2^2 C_{\alpha r} + (l_3 + d_1)^2 C_{\alpha t})(\dot{\epsilon}_r + \dot{\epsilon}_d) \\ +l_3(l_3 + d_1)C_{\alpha t}\dot{\epsilon}_f) + 2(l_3 + d_1)C_{\alpha t}\epsilon_f - m_2 d_3 sin\epsilon_f(\dot{y}_r - \dot{x}\epsilon_r)(\dot{\epsilon}_r + \dot{\epsilon}_d) \\ -2m_2 d_1 d_3 sin\epsilon_f(\dot{\epsilon}_r + \dot{\epsilon}_d)\dot{\epsilon}_f - m_2 d_1 d_3 sin\epsilon_f \dot{\epsilon}_f^2 - m_2(d_1 + d_3 cos\epsilon_f)\dot{x}\dot{\epsilon}_d \\ +(I_{z1} + I_{z2} + m_2 d_1^2 + m_2 d_3^2 + 2m_2 d_1 d_3 cos\epsilon_f)\ddot{\epsilon}_d \end{pmatrix}$$

and

$\Phi(q_r, \dot{q}_r, \dot{\epsilon}_d, \ddot{\epsilon}_d)(3) =$
$$\begin{pmatrix} \frac{2}{\dot{x}}(-l_3 C_{\alpha t}(\dot{y}_r - \dot{x}\epsilon_r) + l_3(l_3 + d_1)C_{\alpha t}(\dot{\epsilon}_r + \dot{\epsilon}_d) + l_3^2 C_{\alpha t}\dot{\epsilon}_f) + m_2 d_3 sin\epsilon_f(\dot{\epsilon}_r + \dot{\epsilon}_d)^2 \\ +2l_3 C_{\alpha t}\epsilon_f - m_2 d_3 sin\epsilon_f(\dot{y}_r - \dot{x}\epsilon_r)(\dot{\epsilon}_r + \dot{\epsilon}_d) - m_2 d_3 cos\epsilon_f \dot{x}\dot{\epsilon}_d + (I_{z2} + m_2 d_3^2 + m_2 d_1 d_3 cos\epsilon_f)\ddot{\epsilon}_d \end{pmatrix}.$$

Eq. (123) is the simplified model which will be used to design the steering control algorithm in section 10 for the lane following maneuver.

9.3 Linear Analysis of the Control Model

The control model (123) can be further linearized by approximating $cos\epsilon_f \simeq 1, sin\epsilon_f \sim \epsilon_f$ and neglecting the second order terms. Then the linearized model has the form

$$M\ddot{q}_r + D\dot{q}_r + Kq_r = F\delta + E_1\dot{\epsilon}_d + E_2\ddot{\epsilon}_d, \tag{124}$$

where $\dot{\epsilon}_d$ and $\ddot{\epsilon}_d$ are exogenous inputs representing the disturbace effects on curved roads. Two interesting properties are observed from this linearized model.

1. M is a symmetric positive definite matrix which contains the inertial information of the vehicle system.

40

2. The D matrix can be interpreted as a damping matrix. Each element of the C matrix contains the tire cornering stiffness. If the cornering stiffness is small, the vehicle system will become lightly damped and more oscillatory. For example, if the vehicle is operated on an icy road, the vehicle stability will decrease. We also see that the vehicle longitudinal velocity x appears in the denominator of the damping matrix. Therefore the system damping is inversely proportional to the vehicle longitudinal velocity, which also agrees with our physical experience.

The first property that M is a positive definite matrix will be exploited in synthesizing the input-output linearizing controller.

10   Steering Control of Tractor-Semitrailer Vehicles

10.1   Controller Design

In this section a steering control algorithm will be designed by applying the input-output linearization scheme (Isidori 1995, Nijmeijer 1990). The steering control model developed in section 9 is

$$M\ddot{q}_r + \Phi(q_r, \dot{q}_r, \dot{\epsilon}_d) = F\delta \tag{125}$$

where M is the inertial matrix and can be partition into four blocks as

$$M = \left(\begin{array}{c|cc} m_1 + m_2 & -m_2(d_1 + d_3) & -m_2 d_3 \\ \hline -m_2(d_1 + d_3) & I_{z1} + I_{z2} + m_2(d_1 + d_3)^2 & I_{z2} + m_2 d_3^2 + m_2 d_1 d_3 \\ -m_2 d_3 & I_{z2} + m_2 d_3^2 + m_2 d_1 d_3 & I_{z2} + m_2 d_3^2 \end{array} \right) \equiv \left(\begin{array}{c|c} M_{11} & M_{12} \\ \hline M_{21} & M_{22} \end{array} \right)$$

Since the matrix M is positive definite, both M_{11} and M_{22} are also positive definite. The control model in (125) can be divided into two subsystems:

$$M_{11}\ddot{y}_r + M_{12} \left(\begin{array}{c} \ddot{\epsilon}_r \\ \ddot{\epsilon}_f \end{array} \right) + \Phi_1 = C_{\alpha f}\delta \tag{126}$$

and

$$M_{21}\ddot{y}_r + M_{22} \left(\begin{array}{c} \ddot{\epsilon}_r \\ \ddot{\epsilon}_f \end{array} \right) + \left(\begin{array}{c} \Phi_2 \\ \Phi_3 \end{array} \right) = \left(\begin{array}{c} l_1 C_{\alpha f} \\ 0 \end{array} \right) \delta. \tag{127}$$

Notice that the second subsystem (127) can be rewritten as

$$\left(\begin{array}{c} \ddot{\epsilon}_r \\ \ddot{\epsilon}_f \end{array} \right) = M_{22}^{-1} \left\{ -M_{21}\ddot{y}_r - \left(\begin{array}{c} \Phi_2 \\ \Phi_3 \end{array} \right) + \left(\begin{array}{c} l_1 C_{\alpha f} \\ 0 \end{array} \right) \delta \right\}. \tag{128}$$

41

Substituting Eq. (128) into Eq. (126), we obtain the input(δ)-output(y_r) dynamics as

$$\bar{M}_{11}\ddot{y}_r + \bar{\bar{\Phi}} = \bar{K}\delta, \tag{129}$$

where

$$\bar{M}_{11} = M_{11} - M_{12}M_{22}^{-1}M_{21}, \tag{130}$$

$$\bar{\bar{\Phi}} = \Phi_1 - M_{12}M_{22}^{-1}\begin{pmatrix} \Phi_2 \\ \Phi_3 \end{pmatrix}, \tag{131}$$

and

$$\bar{K} = C_{\alpha f} - M_{12}M_{22}^{-1}\begin{pmatrix} l_1 C_{\alpha f} \\ 0 \end{pmatrix}. \tag{132}$$

Note that

$$\bar{M}_{11} = T^T M T \tag{133}$$

and

$$T = \begin{pmatrix} I \\ -M_{22}^{-1}M_{21} \end{pmatrix} \tag{134}$$

which is a full rank matrix. By the facts that the matrix M is positive definite and that the matrix T has a full rank, we conclude that $\bar{M}_{11}$ is also positive definite. If $\bar{K} \neq 0$, we can choose the linearizing control law

$$\bar{K}\delta = \bar{M}_{11}v + \bar{\bar{\Phi}} \tag{135}$$

With this linearizing control law, the subsystems (126) and (127) become

$$\ddot{y}_r = v \tag{136}$$

and

$$M_{22}\begin{pmatrix} \ddot{\epsilon}_r \\ \ddot{\epsilon}_f \end{pmatrix} + \begin{pmatrix} \Phi_2 \\ \Phi_3 \end{pmatrix} = (\begin{pmatrix} l_1 C_{\alpha f} \\ 0 \end{pmatrix}\bar{M}_{11} - M_{21})v + \begin{pmatrix} l_1 C_{\alpha f} \\ 0 \end{pmatrix}\bar{\bar{\Phi}} \tag{137}$$

Furthermore, by choosing

$$v = k_d \dot{y}_r + k_p y_r \tag{138}$$

the output y_r converges to zero asymptotically.

42

10.2 Simulation Results

The simulations are conducted using the complex vehicle model and the vehicle parameters are listed in Table 2. The simulation scenario we used is depicted in Fig. **14.** The tractor-semitrailer vehicle travels along a straight roadway with an initial lateral displacement of **15** cm and enters a curved section with a radius of curvature of 450 m at time t $= 5$ sec. Fig. **15** shows the simulation results of the input-output linearization controller at a vehicle speed of 60 MPH. We see that the lateral tracking error converges to zero asymptotically while the yaw angle of the tractor and the relative yaw angle of the trailer are small.
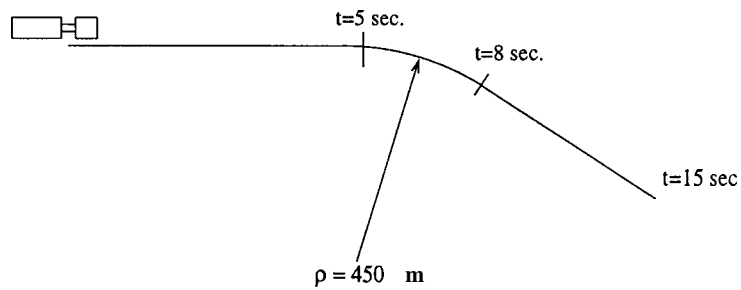

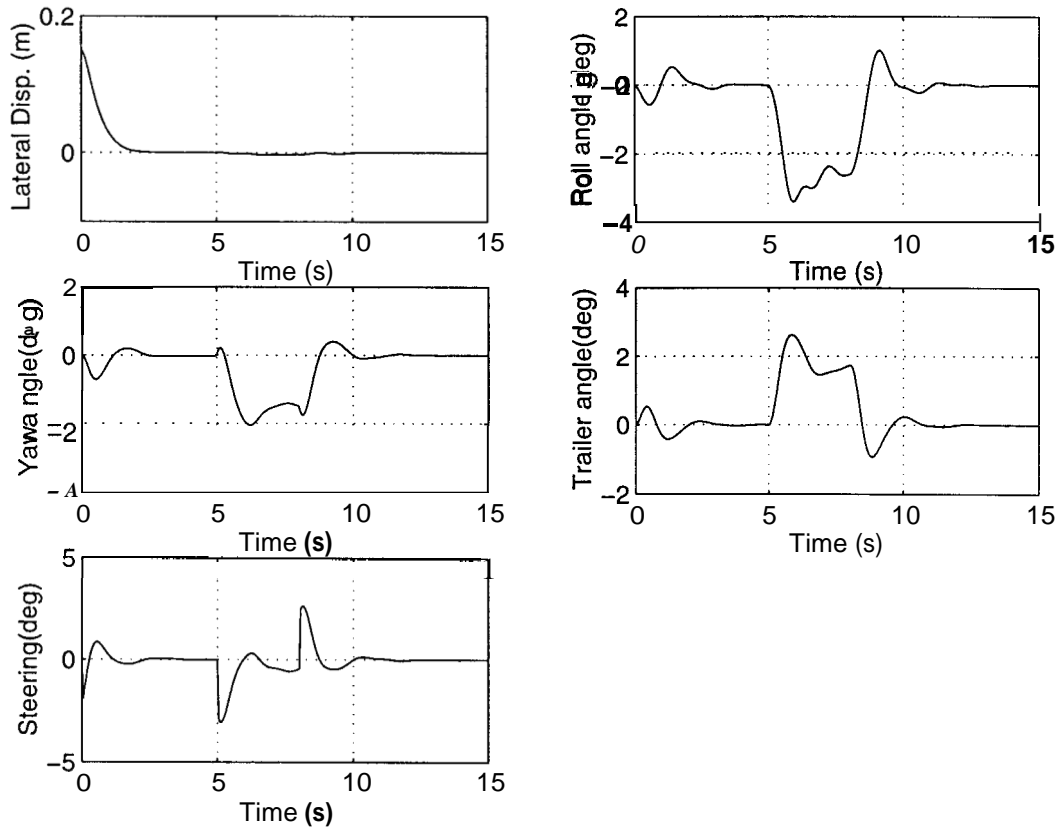Figure **14:** Simulation Scenario

Figure 15: Input/Output Linearization Control

11 Steering and Braking Control Model (SIM2)

In this section, the control model developed in section 9 is reformulated to include the left and right braking forces at the trailer **as** another two control inputs. Recall that in section 9, the simplified vehicle model was obtained **as**

$$
\begin{aligned}
&(m_1 + m_2)\ddot{y}_u - m_2(d_1 + d_3 cos\epsilon_f)\ddot{\epsilon}_1 - m_2 d_3 cos\epsilon_f \ddot{\epsilon}_f \\
&+ (m_1 + m_2)\dot{x}_u \dot{\epsilon}_1 + m_2 d_3 sin\epsilon_f (\dot{\epsilon}_1 + \dot{\epsilon}_f)^2 \\
&= F_{b1} + F_{b2} + F_{b3} + F_{b4} + F_{b5} + F_{b6},
\end{aligned}
\tag{139}
$$

$$
\begin{aligned}
&-m_2(d_1 + d_3 cos\epsilon_f)\ddot{y}_u + (I_{z1} + I_{z2} + m_2(d_1 + d_3 cos\epsilon_f)^2)\ddot{\epsilon}_1 \\
&+ (I_{z2} + m_2 d_3^2 + m_2 d_1 d_3 cos\epsilon_f)\ddot{\epsilon}_f \\
&- m_2(d_1 + d_3 cos\epsilon_f)\dot{x}_u \dot{\epsilon}_1 - m_2 d_3 sin\epsilon_f \dot{y}_u \dot{\epsilon}_1 \\
&- 2m_2 d_1 d_3 sin\epsilon_f \dot{\epsilon}_1 \dot{\epsilon}_f - m_2 d_1 d_3 sin\epsilon_f \dot{\epsilon}_f^2 \\
&= (F_{b1} + F_{b2})l_1 - (F_{b3} + F_{b4})l_2 - (F_{b5} + F_{b6})(d_1 + l_3) \\
&+ (F_{a2} - F_{a1})\frac{T_{w1}}{2} + (F_{a4} - F_{a3})\frac{T_{w2}}{2} + (F_{a6} - F_{a5})\frac{T_{w3}}{2},
\end{aligned}
\tag{140}
$$

and

$$
\begin{aligned}
&-m_2 d_3 cos\epsilon_f \ddot{y}_u + (I_{z2} + m_2 d_3^2 + m_2 d_1 d_3 cos\epsilon_f)\ddot{\epsilon}_1 + (I_{z2} + m_2 d_3^2)\ddot{\epsilon}_f \\
&- m_2 d_3 cos\epsilon_f \dot{x}_u \dot{\epsilon}_1 - m_2 d_3 sin\epsilon_f \dot{y}_u \dot{\epsilon}_1 + m_2 d_1 d_3 sin\epsilon_f \dot{\epsilon}_1^2 \\
&= -(F_{b5} + F_{b6})l_3 + (F_{a6} - F_{a5})\frac{T_{w3}}{2}.
\end{aligned}
\tag{141}
$$

By substituting the linear lateral tire model

$$
F_{bi} = \begin{cases} C_{\alpha_f}\alpha_f & for \ i = 1,2 \\ C_{\alpha_r}\alpha_f & for \ i = 3,4 \\ C_{\alpha_t}\alpha_f & for \ i = 5,6 \end{cases}
$$

into (139), (140) and (141) and assuming the longitudinal tire forces on the tractor are zero, i.e., $F_{a1} = F_{a2} = F_{a3} = F_{a4} = 0$, we obtain the simplified model **as**

$$
M\ddot{q} + C(q, \dot{q}) + D\dot{q} + Kq = H \cdot U
\tag{142}
$$

where **Ad,** $C(q, \dot{q})$, D and K are the same **as** in SIM1, (118), and H and U are

$$
H = \begin{pmatrix} 2C_{\alpha f} & 0 \\ 2l_1 C_{\alpha f} & \frac{T_{w3}}{2} \\ 0 & \frac{T_{w3}}{2} \end{pmatrix}
$$

45

and

$$U = \left(\begin{array}{c} \delta \\ F_{a6} - F_{a5} \end{array} \right) \equiv \left(\begin{array}{c} \delta \\ T \end{array} \right) \tag{143}$$

respectively. Eq. (142) is the model with respect to the unsprung mass reference frame. Parallel to the development of SIM1 in section 9 and by using the coordinate transformations (119) (120) (121) and (122), the steering and braking control model SIM2 with respect to the road reference frame is obtained

$$M(q_r)\ddot{q}_r + \Phi(q_r, \dot{q}_r, \dot{\epsilon}_d, \ddot{\epsilon}_d) = H \cdot U \tag{144}$$

Notice that F_{a5} and F_{a6} in (143) stand for the longitudinal forces at the left and right wheels of the trailer. Thus T is the differential force acting on the trailer. We denote the longitudinal force $F_{ai} < 0$ when it is a braking force and $F_{ai} > 0$ when it is a traction force. In fact, the control inputs F_{a5} and F_{a6} at the wheels of the trailer can only be negative, i.e., we can use only braking instead of traction. This would be a big constraint on the control inputs F_{ai}. However, the differential force T can be both positive and negative. Furthermore, the braking forces F_{a5} and F_{a6} are determined by the tire force model and are functions of the tire slip ratio. Specifically, as shown in Fig. 16, the wheel dynamics are

$$I_w \dot{\omega}_i = -F_{ai} r + \tau_i \tag{145}$$

where ω_i is the angular velocity of the wheel, F_{ai} is the braking force generated at the tire/ground interface, and τ_i is the braking torque applied at the braking disk of the wheel. The tire slip ratio is defined as

$$\lambda_i = \frac{\omega_i r_1 - V}{V} \tag{146}$$

and the braking force is

$$F_{ai} = C_l \lambda_i \tag{147}$$

Eq. (144) as well as Eqs. (145) (146) and (147) will be used to design the coordinated steering and braking control algorithm in section 12.

12   Coordinated Steering and Independent Braking Control

12.1   Controller Design

In this section, a coordinated steering and braking control algorithm will be designed. Motivated by Matsumoto and Tomizuka (1992), we propose to use not only the tractor front wheel steering input but
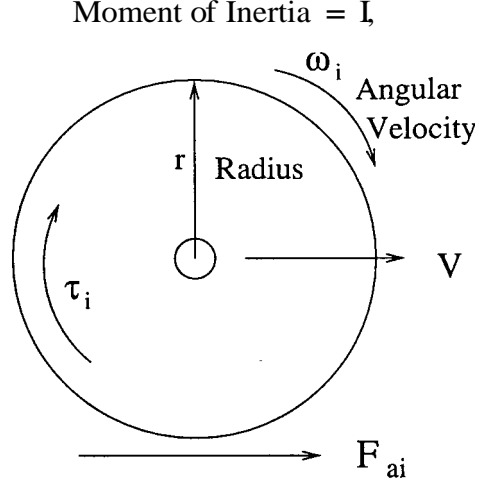
Figure 16: Wheel Dynamics

also the trailer unilateral tire braking to provide the differential torque for directly controlling the trailer yaw motion. The control algorithm will be designed in two steps. In the first step, we assume the differential force T is control input. Then the desired steering command δ_d and the desired differential braking force T_d are determined by input/output linearization scheme. By the nature of unilateral braking, if $T_d > 0$, we have $F_{a5d} = -T_d$ and $F_{a6d} = 0$. On the other hand, if $T_d < 0$, we have $F_{a5d} = 0$ and $F_{a6d} = T_d$. In the second step, the required braking torques τ_5 and τ_6 are determined to generate the desired braking forces F_{a5d} and F_{a6d} by utilizing backstepping design methodologies.

Step 1

First, we define the first system output e_1 **as** the lateral tracking error

$$e_1 = y_r \tag{148}$$

and the second output e2 **as** the articulation angle between the tractor and the trailer

$$e2 = \epsilon_f \tag{149}$$

Differentiating e_1 and e2 twice, we obtain

$$\begin{pmatrix} \ddot{e_1} \\ \ddot{e_2} \end{pmatrix} = \begin{pmatrix} M^{-1}(1) \\ M^{-1}(3) \end{pmatrix} C(\dot{q}, \dot{\epsilon}_d, \ddot{\epsilon}_d) + \begin{pmatrix} M^{-1}(1) \\ M^{-1}(3) \end{pmatrix} HU \tag{150}$$

The number i in the parenthesis $M^{-1}(i)$ denotes the $i-th$ row of the M^{-1} matrix. For notational simplicity, we define

$$J = \begin{pmatrix} M^{-1}(1) \\ M^{-1}(3) \end{pmatrix} H \tag{151}$$

47

If the matrix J is nonsingular, we can choose the control input U as

$$U = -J^{-1} \begin{pmatrix} M^{-1}(1) \\ M^{-1}(3) \end{pmatrix} C(\dot{q}, \dot{\epsilon}_d, \ddot{\epsilon}_d) - J^{-1} \left\{ K_D \begin{pmatrix} \dot{e}_1 \\ \dot{e}_2 \end{pmatrix} + K_P \begin{pmatrix} e_1 \\ e_2 \end{pmatrix} \right\} \tag{152}$$

This control law cancels the system nonlinearities and inserts the desired error dynamics. Thus the closed loop system becomes

$$\begin{pmatrix} \ddot{e}_1 \\ \ddot{e}_2 \end{pmatrix} + K_D \begin{pmatrix} \dot{e}_1 \\ \dot{e}_2 \end{pmatrix} + K_P \begin{pmatrix} e_1 \\ e_2 \end{pmatrix} = 0. \tag{153}$$

Step 2

In _Step_ 1 we regard T as a real control input; then the desired steering command and the desired differential braking forces T_d are set in (152). In this step we will 'backstep' to determine the braking torques τ_5 and τ_6 on the trailer's left and right wheels. Recall that the wheel dynamics is

$$I_w \dot{\omega}_i = -F_{ai} r + \tau_i \tag{154}$$

and the tire force is

$$F_{ai} = C_{lt} \lambda_i \tag{155}$$

where the slip ratio λ_i is defined as

$$\lambda_i = \frac{\omega_i r - V}{V} \tag{156}$$

Combining equations (154), (155) and (156), we obtain

$$\begin{aligned} F_{ai} &= C_{lt} \lambda_i \\ &= C_{lt}(\tfrac{\partial \lambda_i}{\partial V}\dot{V} + \tfrac{\partial \lambda_i}{\partial \omega_i}\dot{\omega}_i) \\ &= C_{lt}(-\tfrac{\omega_i r}{V^2}\dot{V} + \tfrac{r}{I_w V}(-C_{lt}\lambda_i r + \tau_i)) \end{aligned} \tag{157}$$

Thus the equations governing the vehicle dynamics and wheel dynamics are

$$\begin{pmatrix} \ddot{e}_1 \\ \ddot{e}_2 \end{pmatrix} = \begin{pmatrix} M^{-1}(1) \\ M^{-1}(3) \end{pmatrix} C(\dot{q}, \dot{\epsilon}_d, \ddot{\epsilon}_d) + J \cdot U \tag{158}$$

and

$$\dot{F}_{ai} = C_{lt}(-\tfrac{\omega_i r}{V^2}\dot{V} + \tfrac{r}{I_w V}(-C_{lt}\lambda_i r + \tau_i)) \tag{159}$$

Recall that $T = F_{a6} - F_{a5}$ and both F_{a5} and F_{a6} are negative. In this unilateral braking scheme, if T_d determined in (152) is positive, we have $F_{a5d} = -T_d$ and $F_{a6d} = 0$. Thus the braking controller will apply the brake torque on the trailer left wheel. On the other hand, if T_d is negative, we have $F_{a5d} = 0$ and $F_{a6d} = T_d$, so the braking controller will apply the brake torque on the trailer right wheel. From Eq. (152) in *step 1,* the control inputs are chosen **as**

$$\delta = \delta_d(q_r, \dot{q}_r, \dot{\epsilon}_d) \tag{160}$$

and

$$T = T_d(q_r, \dot{q}_r, \dot{\epsilon}_d) \tag{161}$$

such that the error dynamics becomes

$$\ddot{e}_1 + k_{d1}\dot{e}_1 + k_{p1}e_1 = 0 \tag{162}$$

and

$$\ddot{e}_2 + k_{d2}\dot{e}_2 + k_{p2}e_2 = 0. \tag{163}$$

Note that T is determined by the braking force F_{ai}, and that braking force F_{ai} can be adjusted only through equation (159), i.e., the braking torque τ_i is the actual control input. Therefore, T cannot be simply set to T_d all the time, and τ_i must be adjusted so that the difference between T_d and T is brought to zero. This is the main idea in the backstepping procedure, We define two new variables η_1 and η_2 **as**

$$\eta_1 = F_{a5} - F_{a5d} \tag{164}$$

and

$$\eta_2 = F_{a6} - F_{a6d}, \tag{165}$$

respectively. Then we have

$$\begin{aligned} T &= F_{a6} - F_{a5} \\ &= F_{a6d} + \eta_2 - F_{a5d} - \eta_1 \\ &= T_d + \eta_2 - \eta_1. \end{aligned} \tag{166}$$

Noting

$$\begin{aligned} \dot{\eta}_1 &= \dot{F}_{a5} - \dot{F}_{a5d} \\ &= C_{lt}(-\tfrac{\omega_5 r}{V^2}\dot{V} + \tfrac{r}{I_w V}(-C_{lt}\lambda_5 r + \tau_5)) - \dot{F}_{a5d} \end{aligned} \tag{167}$$

and

$$\begin{aligned} \dot{\eta}_2 &= \dot{F}_{a6} - \dot{F}_{a6d} \\ &= C_{lt}(-\tfrac{\omega_6 r}{V^2}\dot{V} + \tfrac{r}{I_w V}(-C_{lt}\lambda_6 r + \tau_6)) - \dot{F}_{a6d}, \end{aligned} \tag{168}$$

we choose

$$\tau_5 = C_{lt}\lambda_5 r + \frac{I_w V}{r}\left(-\frac{\omega_5 r}{V^2}\dot{V} + \frac{1}{C_{lt}}(\dot{F}_{a5d} - k_1\eta_1)\right) \tag{169}$$

and

$$\tau_6 = C_{lt}\lambda_6 r + \frac{I_w V}{r}\left(-\frac{\omega_6 r}{V^2}\dot{V} + \frac{1}{C_{lt}}(\dot{F}_{a6d} - k_2\eta_2)\right). \tag{170}$$

Then, we obtain

$$\ddot{e}_1 + k_{d1}\dot{e}_1 + k_{p1}e_1 + J_{12}(\eta_2 - \eta_1) = 0, \tag{171}$$

$$\ddot{e}_2 + k_{d2}\dot{e}_2 + k_{p2}e_2 + J_{22}(\eta_2 - \eta_1) = 0, \tag{172}$$

$$\dot{\eta}_1 + k_1\eta_1 = 0, \tag{173}$$

and

$$\dot{\eta}_2 + k_2\eta_2 = 0, \tag{174}$$

where J_{12} and J_{22} are the $(1,2)$ and $(2,2)$ elements of the matrix J. Defining the state vector $(x_1, x_2, x_3, x_4)^T$ as $(e_1, \dot{e}_1, e_2, \dot{e}_2)^T$ and transforming equations (171) and (172) to state space form, we have

$$\frac{d}{dt}\begin{pmatrix} x_1 \\ x_2 \\ x_3 \\ x_4 \end{pmatrix} = \begin{pmatrix} 0 & 1 & 0 & 0 \\ k_{p1} & k_{d1} & 0 & 0 \\ 0 & 0 & 1 & 0 \\ 0 & 0 & k_{p2} & k_{d2} \end{pmatrix}\begin{pmatrix} x_1 \\ x_2 \\ x_3 \\ x_4 \end{pmatrix} + \begin{pmatrix} 0 & 0 \\ J_{12} & -J_{12} \\ 0 & 0 \\ J_{22} & -J_{22} \end{pmatrix}\begin{pmatrix} \eta_1 \\ \eta_2 \end{pmatrix} \tag{175}$$

Then the overall system can be rewritten as

$$\frac{d}{dt}\begin{pmatrix} x_1 \\ x_2 \\ x_3 \\ x_4 \\ \hline \eta_1 \\ \eta_2 \end{pmatrix} = \left(\begin{array}{cccc|cc} 0 & 1 & 0 & 0 & 0 & 0 \\ -k_{p1} & -k_{d1} & 0 & 0 & J_{12} & -J_{12} \\ 0 & 0 & 0 & 1 & 0 & 0 \\ 0 & 0 & -k_{p2} & -k_{d2} & J_{22} & -J_{22} \\ \hline 0 & 0 & 0 & 0 & -k_1 & 0 \\ 0 & 0 & 0 & 0 & 0 & -k_2 \end{array}\right)\begin{pmatrix} x_1 \\ x_2 \\ x_3 \\ x_4 \\ \hline \eta_1 \\ \eta_2 \end{pmatrix} \tag{176}$$

We see that the overall system matrix can be divided by four blocks and the lower off-diagonal block is identically zero. Thus the eigenvalues of the overall system are the union of those of the block diagonal matrices. Since each block diagonal matrix is asymptotically stable, the overall system is asymptotically stable.

12.2 Simulation Results

We use the same scenario shown in Fig.14. Vehicle longitudinal speed is 26.4 m/s (60 MPH). Figs. 17 and 18 show the simulation results of the coordinated steering and independent braking control. Notice that in implementing this control algorithm, we impose upper and lower bounds on the braking torque input to avoid tire force saturation. Comparison of the steering control designed in section 10 and the coordinated steering and independent braking control is shown in Fig. 19, from which we see that the peak trailer yaw errors are reduced from 2.64^0 to 0.97^0. We also observe that the longitudinal velocity decreases when the independent braking control algorithm is activated. **As** we stated in section 9.3 that the system damping is inversely proportional to the longitudinal velocity, so a decrease of the longitudinal velocity will contribute to decreases of both tractor and trailer yaw errors. To see the effect caused only by the differential forces distribution over the inner and outer tires of the trailer, we assume that the longitudinal controller will give traction force commands on the tractor to counteract the braking forces on the trailer. Simulation results for this scenario is given in Fig. 20 , which shows that the trailer yaw errors is reduced from 2.64' to 1.13'. Recall from Table 2 that the length of the trailer is 9.65 m. Thus a decrease of 1.51' in yaw errors corresponds to a decrease of 25.4 cm in lateral tracking errors of the trailer.
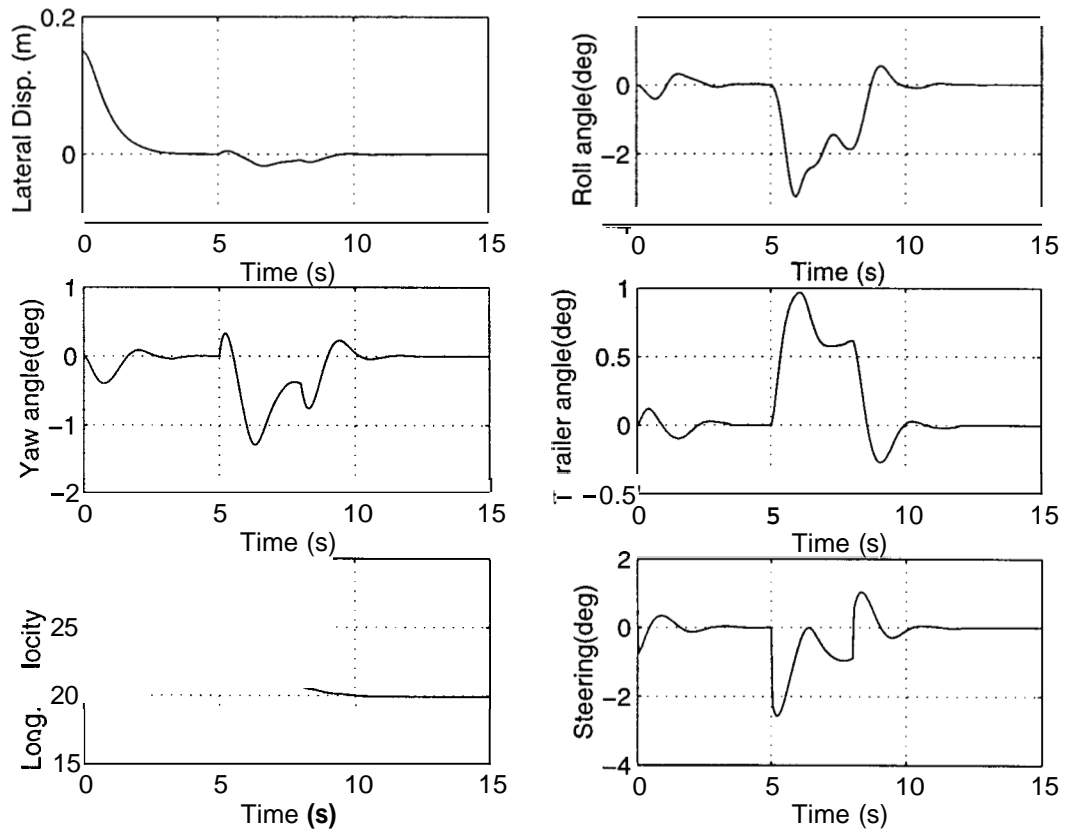
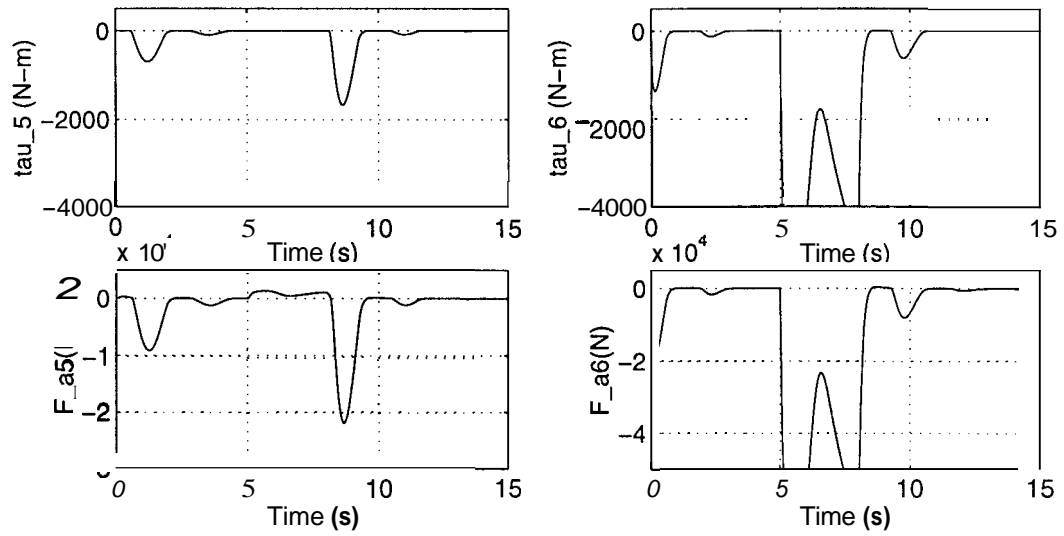Figure 17: Input/Output Linearization Control with Trailer Independent Braking

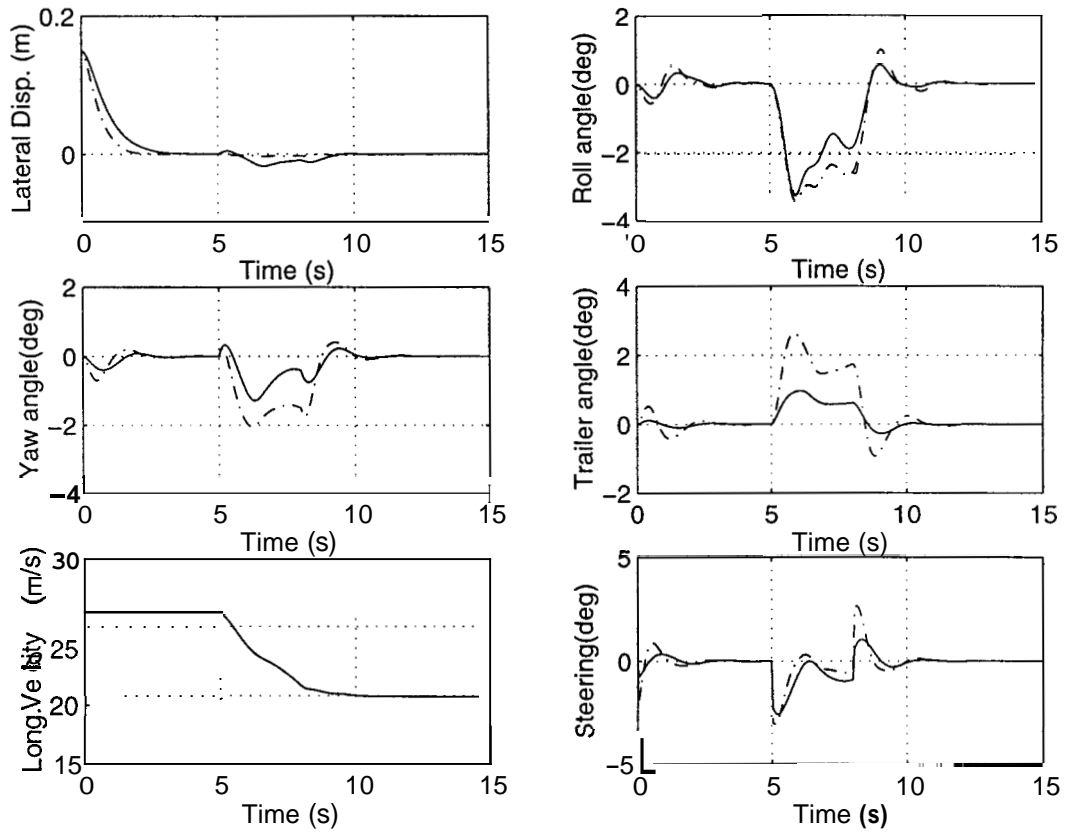Figure 18: Input/Output Linearization Control with Trailer Independent Braking

Figure 19: Comparison of input/output linearization control with (solid line) and without (dashdot line) trailer independent braking
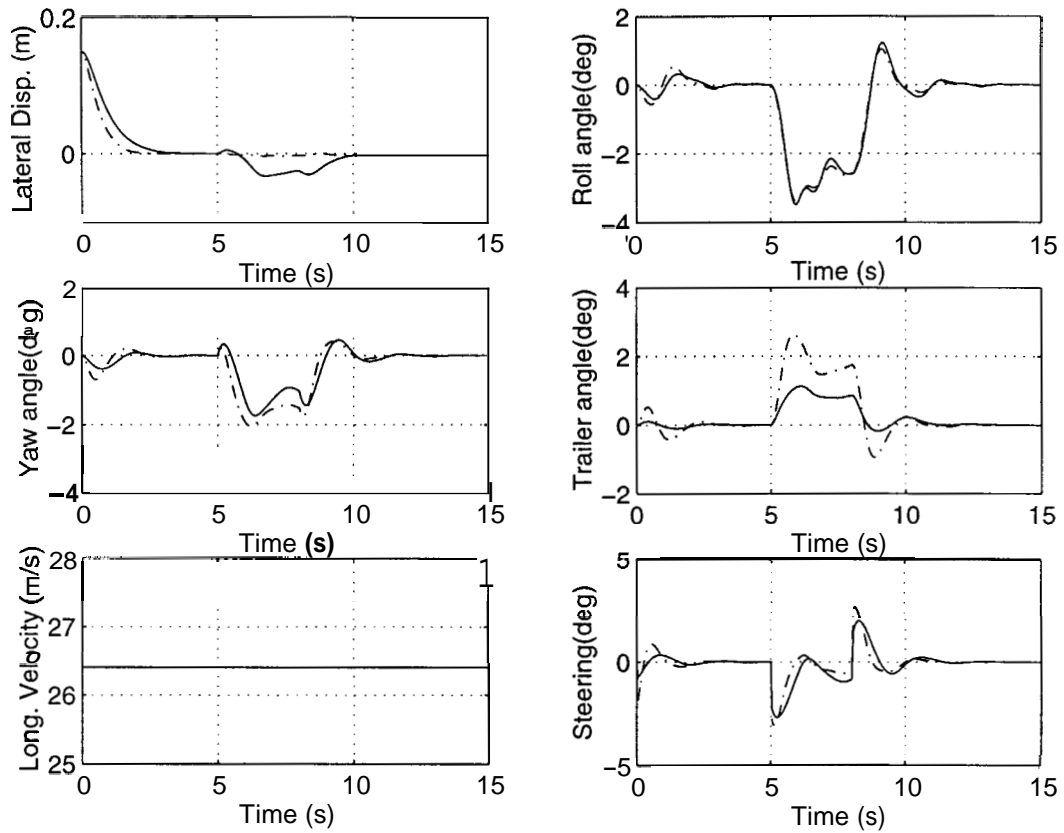
Figure 20: Comparison of input/output linearization control with (solid line) and without (dashdot line) trailer independent braking when the longitudinal speed is constant

13 Conclusions

Two types of dynamic models of tractor-semitrailer vehicles are utilized for the design and analysis of lateral controllers. The first type of dynamic model is a complex simulation model. The second type of dynamic models are two simplified control models, which will be derived from the complex nonlinear model. This modeling approach utilizes Lagrangian mechanics and has an advantage over a Newtonian mechanics formulation in that this complex model eliminates the holonomic constraint at the fifth wheel (linking joint) by choosing the generalized coordinates. Since there is no constraint involved in the equations of motion, it is easier to design control algorithms and to solve the differential equations numerically. The effectiveness of this modeling approach was shown by comparing the experimental results of a tractor-semitrailer vehicle and the simulation results of the complex tractor-semitrailer vehicle model.

Two control algorithms for lateral guidance of tractor-semitrailer vehicles were designed. The first was a baseline steering control algorithm and the second was a coordinated steering and independent braking control algorithm. In the design of the second control algorithm, we utilized tractor front wheel steering angles and trailer independent braking forces to control the tractor and the trailer motion. The multivariable backstepping design methodology developed in (Chen and Tomizuka 1997) was utilized to determine the coordinated steering angle and braking torques on the trailer wheels. Simulations showed that both the tractor and the trailer yaw errors under coordinated steering and independent braking force control were smaller than those without independent braking force control.

References

[1] Bishel, R. A. 1993. "Dual-Mode Truck: Automated and Manual Operation", *SAE technical paper series, number **931837**,* August 1993.

[2] Baraket, Z., and P. Fancher. 1989. "Representation of Truck Tire Properties in Braking and Handling Studies: The Influence of Pavement and Tire Conditions on Frictional Characteristics", Technical Report, University of Michigan, Ann Arbor, UMTRI-89-33, 1989.

[3] Chen, C., and M. Tomizuka. 1995. "Steering and Independent Braking Control of Tractor-Semitrailer Vehicles in Automated Highway Systems", *Proc. of IEEE Conference on Decision and Control,* New Orleans, 1995.

[4] Chen, C., and M. Tomizuka. 1997. "Control of Multivariable Nonlinear Systems without Vector Relative Degrees: A Backstepping Approach", *Proc. of IEEE Conference on Decision and Control,* San Diego, 1997.

[5] Favre, B. 1995. "The Position of a Truck Manufacturer Regarding Intelligent Transportation Systems Advanced Technologies", *proceedings of the University of California/PATH - France Workshop,* 24-25th October 1995, California PATH, Richmond, CA.

[6] Fenton, R. E., and R. J. Mayhan. 1991. "Automated Highway Studies at The Ohio State University-An Overview", *IEEE Transactions on Vehicular Technology,* vol. VT-40, no. 1, Feb. 1991, pp. 100-113.

[7] Greenwood, D. T. 1977. *Classical Dynamics,* Prentice Hall, 1977.

[8] "Highway statistics, 1993, 49th ed." 1994. Federal Highway Administration, 1994.

[9] Isidori, A. 1995. *Nonlinear Control Systems, 3rd Ed.,* Springer, 1995.

[10] Kanellakopoulos, I., and M. Tomizuka. 1996. "Commercial Trucks and Buses in Automated Highway Systems," in *Automated Highway Systems,* edited by P. Ioannou, Plenum Publishing Corporation, 1996.

[11] Matsumoto, N., and M. Tomizuka. 1992. "Vehicle Lateral Velocity and Yaw Rate Control With Two Independent Control Inputs", *ASME J. of Dynamical Systems, Measurement, and Control,* Vol. 114, 1992.

[12] *Motor Vehicles Facts and Figures.* 1993. American Automobile Manufacturers' Association, 1993.

[13] Nijmeijer, H., and A.J. van der Schaft. 1990. *Nonlinear Dynamical Control Systems,* Springer-Verlag, 1990.

[14] Pacejka, H. B., and E. Bakker. 1991. "The Magic Formula Tire Model", *proceedings of 1st International Colloquium on Tire Models for Vehicle Dynamics Analysis, Deft, The Netherlands, October 1991,*

[15] Peng, H. and M. Tomizuka. 1993. "Preview Control for Vehicle Lateral Guidance in Highway Automation," *ASME Journal of Dynamic Systems, Measurement and Control,* Vol. 115, No. 4, pp. 678-686.

[16] Rosenberg, R. M. 1977. *Analytical Dynamics of Discrete Systems,* Plenum Press, 1977

[17] Shladover, S. et. al. 1991. "Automatic Vehicle Control Developments in the PATH Program", *IEEE Transactions on Vehicular Technology,* vol. VT-40, no. 1, Feb. 1991, pp. 114-130.

[18] Yanakiev, D., and I. Kanellakopoulos. 1995. "Analysis, Design and evaluation of AVCS for Heavy Duty Vehicles: Phase 1 Report" *California PATH working paper UCB-ITS-PWP-95-12,* 1995.

[19] Zimmermann, T., A. Fuchs, U. Franke and B. Klingenberg. 1994. "VECTOR -A Vision Enhanced/Controlled Truck for Operational Research", *SAE technical paper series, number 942284,* November, 1994.